

Learning Theory of Transformers: Local-to-Global Approximation via Softmax Partition of Unity

Zhongjie Shi ^{*} and Wenjing Liao [†]

Abstract

This paper investigates the learning theory of Transformer networks for regression tasks on the compact Euclidean domain $[0, 1]^d$ and d -dimensional compact Riemannian manifolds. We propose a novel constructive approximation framework for Transformers that builds local approximations of the target function and aggregates them into a global approximation via softmax partition of unity. This approach leverages the attention mechanism to achieve spatial localization through affine transformations of the input. The softmax activation plays a crucial role in aggregating local approximations to a global output. From an approximation perspective, we prove that a dense Transformer equipped with only two encoder blocks and standard single-hidden-layer point-wise feed-forward networks can achieve a uniform ε -approximation error for α -Hölder continuous functions with $\alpha \in (0, 1]$ using $\mathcal{O}(\varepsilon^{-d/\alpha})$ total parameters. Building upon this approximation guarantee, we establish a near minimax-optimal generalization error bound of order $\mathcal{O}(n^{-\frac{2\alpha}{2\alpha+d}} \log n)$ for the empirical risk minimizer, where n is the training data size. The Transformer architecture studied in this paper is dense, shallow and wide, and employs softmax activation and sinusoidal positional encodings, closely reflecting practical implementations.

1 Introduction

During the past decade, deep learning has achieved remarkable success in various domains, including natural language processing [16, 43, 26], computer vision [22, 15, 40], and complex games [39]. As a leading architecture, the Transformer [43] has become central to these advancements: Vision Transformers (ViTs) have surpassed classical convolutional networks in image recognition [10], while large language models (LLMs) demonstrate exceptional generative and reasoning abilities [2, 31]. Despite this widespread empirical success, the theoretical understanding of the expressivity and generalization capability of the Transformers remains limited.

To establish a learning theory of Transformers, extensive research has investigated their expressivity and generalization. Initial studies focused on universal approximation properties, demonstrating that various Transformer models can universally approximate continuous (permutation equivariant) sequence-to-sequence functions [47, 48, 49, 21]. Beyond universality, inspired by the constructive techniques developed for classical deep ReLU networks [45, 32, 37], recent studies have shown that Transformers can achieve satisfying approximation bounds and has the potential to overcome the curse of dimensionality under certain structural assumptions [17, 41, 19, 18, 36, 20].

^{*}School of Mathematics, Georgia Institute of Technology, Atlanta, GA 30332, United States; E-mail: zshi332@gatech.edu

[†]School of Mathematics, Georgia Institute of Technology, Atlanta, GA 30332, United States; E-mail: wliao60@gatech.edu

Based on these approximation results, further studies have provided generalization analysis and statistical rates. These works evaluate sample complexity and estimation errors in different theoretical settings [50, 11, 17, 44, 41, 18, 38, 35, 36]. However, despite these theoretical advances, a clear understanding of the specific role the softmax attention mechanism plays in the expressivity of transformer networks remains elusive, uncovering how this attention mechanism facilitates efficient feature representation learning is still an important problem.

In deep neural network approximation theory [45, 46, 32], a standard local-to-global approach to uniformly approximate α Hölder continuous functions $g : \mathcal{X} \subseteq [0, 1]^d \rightarrow \mathbb{R}$ involves partitioning the domain into explicit meshes to smoothly aggregate local expert approximations. This aggregation necessitates a Partition of Unity (POU). For ReLU feed-forward neural networks (FFNs), constructing a compactly supported POU faces structural bottlenecks due to the piecewise linear activation. Existing constructive proofs generally adopt two paradigms. For $\alpha \in (0, 1]$, the Spike POU method [46] constructs piecewise linear simplex triangulations by composing ReLUs to compute the multivariate minimum of affine mappings, requiring a network depth of $d^2 + d$. The second paradigm constructs the POU through tensor products of one-dimensional trapezoidal functions when they studied high-order Hölder functions [45, 32]. Because ReLU cannot natively compute multiplications, evaluating these products requires deep compositions with a depth of $\mathcal{O}(\log(1/\varepsilon))$ to achieve an ε -accuracy. Fundamentally, both ReLU-based POUs rely on explicit geometric partitions. This reliance on explicit Cartesian grids hinders their generalization to complex geometries such as compact manifolds. Transformer analyses that rely on these ReLU-based POUs inevitably inherit these domain limitations or depth requirements dependent on ε [17, 41, 19, 18, 36, 20]. This leaves the potential representational capacity of the softmax attention mechanism in Transformer architectures underexplored.

To overcome these structural limitations, we propose a novel mesh-free local-to-global constructive approximation framework via Softmax POU. Instead of explicit geometric partitions, our method employs an implicit and smooth mechanism to dynamically allocate weights of local expert approximations, which naturally aligns with the Transformer attention mechanism equipped with softmax activation. Specifically, to approximate a target function $g : \mathcal{X} \rightarrow \mathbb{R}$, we cover the input domain \mathcal{X} with ℓ_2 balls of radius r_g centered at a discrete set of points $\{\mathbf{c}_i\}_{i=1}^{C_g}$. Given a scaling parameter $M_g > 0$, we define the spatially localized weights as

$$\beta_i(\mathbf{x}) = \frac{\exp(M_g(r_g^2 - \|\mathbf{x} - \mathbf{c}_i\|_2^2))}{\sum_{k=1}^{C_g} \exp(M_g(r_g^2 - \|\mathbf{x} - \mathbf{c}_k\|_2^2))} = \frac{\exp(2M_g\langle \mathbf{x}, \mathbf{c}_i \rangle - M_g\|\mathbf{c}_i\|_2^2)}{\sum_{k=1}^{C_g} \exp(2M_g\langle \mathbf{x}, \mathbf{c}_k \rangle - M_g\|\mathbf{c}_k\|_2^2)}. \quad (1)$$

The target function g is then approximated by the convex combination of its values at these discrete centers: $\hat{g}(\mathbf{x}) = \sum_{i=1}^{C_g} \beta_i(\mathbf{x})g(\mathbf{c}_i)$. This Softmax POU functions as a globally supported yet highly localized smooth mesh-free gating mechanism by unifying three fundamental properties: Geometrically, relying purely on the Euclidean distance $\|\mathbf{x} - \mathbf{c}_i\|_2^2$ to the unstructured centers, the Softmax POU completely bypasses the need for explicit grid construction. This mesh-free property enables it to naturally adapt to complex geometries such as Riemannian manifolds. Mechanically, the Softmax POU operates dynamically rather than statically to achieve spatial localization. In contrast to ReLU POUs where the assigned weight depends solely on the absolute distance to a specific grid vertex, the weight in Softmax POU is determined by the relative distance to all available centers \mathbf{c}_k , thereby inherently establishing a global attention competition. Algebraically, softmax activation not only enforces the exact POU condition $\sum_{i=1}^{C_g} \beta_i(\mathbf{x}) = 1$, but also cancels the input-dependent quadratic term $\|\mathbf{x}\|_2^2$. This algebraic cancellation reduces the non-linear distance computation to

purely affine transformations, converting it into the native dot-product attention. Together, these properties reveal an intrinsic structural alignment, empowering shallow Transformers to natively aggregate local approximations via softmax attention and adapt to complex geometries.

Building upon these insights, this paper provides a comprehensive theoretical analysis of the expressive power and generalization capabilities of Transformers. Our main contributions are summarized as follows

- **Softmax POU Approximation Framework.** We propose a novel local-to-global constructive approximation framework based on a globally supported Softmax POU. By algebraically canceling input-dependent quadratic terms, this mesh-free POU mechanism translates relative Euclidean distances into purely affine transformations, inherently establishing a dynamic global attention competition to achieve spatial localization. This exact structural correspondence empowers shallow Transformers to seamlessly fuse localized approximations into an aggregated global approximation via native softmax dot-product attention mechanism.
- **Learning on Euclidean Domains via Softmax POU.** Applying this framework to compact Euclidean spaces $[0, 1]^d$, we constructively prove that a shallow (only two encoder blocks with standard single-hidden-layer FFNs), wide, and dense Transformer with softmax activation and sinusoidal positional encodings achieves a uniform ε -approximation error for α -Hölder continuous functions using $\mathcal{O}(\varepsilon^{-d/\alpha})$ parameters (see Theorem 1). Building upon this, we establish a near minimax-optimal convergence rate of $\mathcal{O}(n^{-\frac{2\alpha}{2\alpha+d}} \log n)$ (see Theorem 2), formally validating the inherent statistical efficiency of the native Transformer architecture without relying on artificial sparsity or structural depth constraints.
- **Adaptivity to Riemannian Manifolds.** We extend our theoretical guarantees to target functions defined on d -dimensional compact Riemannian manifolds embedded in $\mathbb{R}^{\bar{d}}$. We formally prove that by operating directly on the ambient Euclidean metric, the Softmax POU framework natively adapts to such complex geometries. Consequently, shallow Transformers can achieve a uniform ε -approximation error using $\mathcal{O}(\varepsilon^{-d/\alpha})$ parameters (see Theorem 3) and a near minimax-optimal convergence rate of $\mathcal{O}(n^{-\frac{2\alpha}{2\alpha+d}} \log n)$ (see Theorem 4). Because these bounds scale exclusively with the intrinsic dimension d rather than the ambient dimension \bar{d} , our analysis establishes the native Transformer architecture’s inherent capacity to adapt to complex geometries and overcome the curse of dimensionality.

The remainder of this paper is organized as follows: Section 2 defines the Transformer architecture and its hypothesis space. Section 3 establishes the theoretical guarantees on compact Euclidean domains: Subsection 3.1 introduces the Softmax POU framework to prove uniform approximation bounds, and Subsection 3.2 leverages these results to derive generalization rates. Section 4 extends this framework to compact Riemannian manifolds, demonstrating the architecture’s adaptivity to complex geometries and its ability to avoid the curse of dimensionality. Section 5 discusses related literature, and Section 6 concludes the paper. All detailed proofs are deferred to the Appendix.

Notation. We use lower case bold letters for vectors (\mathbf{x}, \mathbf{y}) , upper case bold for matrices (\mathbf{X}, \mathbf{A}) , and calligraphic letters for sets and spaces $(\mathcal{M}, \mathcal{H})$. For a vector \mathbf{x} , $\|\mathbf{x}\|_p$ denotes its standard ℓ_p norm, and $\langle \mathbf{x}, \mathbf{y} \rangle$ denotes the Euclidean inner product. For a matrix \mathbf{X} , $\text{vec}(\mathbf{X})$ denotes its column-wise vectorization, $\|\mathbf{X}\|_{\max} = \max_{i,j} |\mathbf{X}_{i,j}|$ denotes the maximum absolute value among

its elements. For a function $f : \mathcal{X} \rightarrow \mathbb{R}$, $\|f\|_\infty := \sup_{\mathbf{x} \in \mathcal{X}} |f(\mathbf{x})|$ denotes its supremum norm. Let $\mathcal{B}(\mathbf{c}, r)$ and $\bar{\mathcal{B}}(\mathbf{c}, r)$ denote the open and closed Euclidean balls centered at \mathbf{c} with radius r , respectively. We define $[n] := \{1, \dots, n\}$. The Kronecker delta $\delta_{i,j}$ evaluates to 1 if $i = j$ and 0 otherwise.

2 Transformer architecture

In this section, we formally introduce the structure of the Transformer model. The architecture consists of a pre-processing stage followed by L blocks of Transformer encoders. Each encoder block comprises a multi-head attention (MHA) layer, followed by a point-wise FFN layer.

For an input vector $\mathbf{x} \in \mathbb{R}^d$, the pre-processing step $\mathcal{P} : \mathbb{R}^d \rightarrow \mathbb{R}^{D \times P}$ converts the input to an initial hidden representation $\mathbf{Z}_0 \in \mathbb{R}^{D \times P}$ through an affine embedding and the addition of a positional encoding (PE) $\mathbf{P} \in \mathbb{R}^{D \times P}$. Formally, the pre-processing operation is defined as

$$\mathbf{Z}_0 = \mathcal{P}(\mathbf{x}) = (\mathbf{W}_E \mathbf{x} + \mathbf{b}_E) \mathbf{e}_1^\top + \mathbf{P},$$

where $\mathbf{W}_E \in \mathbb{R}^{D \times d}$ is the embedding weight matrix, $\mathbf{b}_E \in \mathbb{R}^D$ is the bias vector, and $\mathbf{e}_1 = [1, 0, \dots, 0]^\top \in \mathbb{R}^P$ is the canonical basis vector that assigns the embedded input exclusively to the first token position. Here, $P \geq 1$ denotes the total sequence length, implying that the remaining $P - 1$ columns of \mathbf{Z}_0 serve as appended padding or latent tokens. We use sinusoidal positional encodings in our constructions, which aligns with the Transformer architectures in practical applications [43].

Consider the i -th encoder block with input $\mathbf{Z}_{i-1} = [z_{i-1}^1, \dots, z_{i-1}^P] \in \mathbb{R}^{D \times P}$. Within the MHA layer $\mathcal{A}_i : \mathbb{R}^{D \times P} \rightarrow \mathbb{R}^{D \times P}$ with H_i heads, each head includes a query matrix $\mathbf{Q}_i^h \in \mathbb{R}^{d_k \times D}$, a key matrix $\mathbf{K}_i^h \in \mathbb{R}^{d_k \times D}$, and a value matrix $\mathbf{V}_i^h \in \mathbb{R}^{d_v \times D}$, where d_k is the uniform query/key dimension and d_v is the uniform value dimension. For $h \in [H_i]$, the output of the h -th attention head $\text{head}_i^h \in \mathbb{R}^{d_v \times P}$ is computed as

$$\text{head}_i^h = \mathbf{V}_i^h \mathbf{Z}_{i-1} \mathbf{A}_i^h,$$

where $\mathbf{A}_i^h \in \mathbb{R}^{P \times P}$ is the attention probability matrix. Its j -th column is defined by

$$(\mathbf{A}_i^h)_{:,j} := \text{Softmax} \left(\left(\mathbf{Z}_{i-1}^\top \mathbf{K}_i^h \mathbf{Q}_i^h \mathbf{Z}_{i-1} \right)_{:,j} \right), \quad j \in [P],$$

with the $\text{Softmax} : \mathbb{R}^P \rightarrow \mathbb{R}^P$ operator applied component-wise as

$$\text{Softmax}(\mathbf{x}) = \left[\frac{e^{x_1}}{\sum_{l=1}^P e^{x_l}}, \dots, \frac{e^{x_P}}{\sum_{l=1}^P e^{x_l}} \right]^\top.$$

To preserve the distinct representations from different heads, the final output of the MHA layer $\hat{\mathbf{Z}}_i \in \mathbb{R}^{D \times P}$ is generated by concatenating the outputs of all H_i heads along the feature dimension, followed by a linear projection

$$\hat{\mathbf{Z}}_i = \mathbf{W}_i^O \begin{bmatrix} \text{head}_i^1 \\ \vdots \\ \text{head}_i^{H_i} \end{bmatrix},$$

where $\mathbf{W}_i^O \in \mathbb{R}^{D \times (H_i \cdot d_v)}$ is the output projection matrix.

The output $\widehat{\mathbf{Z}}_i = [\widehat{\mathbf{z}}_i^1, \dots, \widehat{\mathbf{z}}_i^P] \in \mathbb{R}^{D \times P}$ is subsequently fed into a point-wise FFN. The FFN layer $\mathcal{F}_i : \mathbb{R}^{D \times P} \rightarrow \mathbb{R}^{D \times P}$ with weight matrices $\mathbf{W}_i^1 \in \mathbb{R}^{d_{\#} \times D}$, $\mathbf{W}_i^2 \in \mathbb{R}^{D \times d_{\#}}$ and biases $\mathbf{b}_i^1 \in \mathbb{R}^{d_{\#}}$, $\mathbf{b}_i^2 \in \mathbb{R}^D$ computes

$$\mathbf{z}_i^j = \mathbf{W}_i^2 \sigma \left(\mathbf{W}_i^1 \widehat{\mathbf{z}}_i^j + \mathbf{b}_i^1 \right) + \mathbf{b}_i^2, \quad j \in [P], \quad (2)$$

where $\sigma(\cdot) = \max(0, \cdot)$ is the ReLU activation function applied component-wise.

Finally, for the Transformer model with L encoder blocks, its output is

$$\mathcal{T}_L(\mathbf{x}) = \mathcal{F}_L \circ \mathcal{A}_L \circ \dots \circ \mathcal{F}_1 \circ \mathcal{A}_1 \circ \mathcal{P}(\mathbf{x}) \in \mathbb{R}^{D \times P}.$$

The scalar output is then obtained by reading out the relevant components of $\mathcal{T}_L(\mathbf{x})$, via a linear affine mapping $\mathbf{c}_{L+1}^\top \text{vec}(\mathcal{T}_L(\mathbf{x}))$. With the complete architecture established, we now define the function class expressed by such Transformer networks.

Definition 1 (Transformer Network Class). *For depth $L \in \mathbb{N}$, embedding dimension $D \in \mathbb{N}$, sequence length $P \in \mathbb{N}$, layer configurations $\{H^\ell\}_{\ell=1}^L, \{d_k^\ell\}_{\ell=1}^L, \{d_v^\ell\}_{\ell=1}^L, \{d_{\text{ff}}^\ell\}_{\ell=1}^L \subset \mathbb{N}$, and parameter magnitude bound $M > 0$, we define the class of Transformer networks as*

$$\begin{aligned} & \mathcal{T} \left(L, D, P, \{H^\ell\}_{\ell=1}^L, \{d_k^\ell\}_{\ell=1}^L, \{d_v^\ell\}_{\ell=1}^L, \{d_{\text{ff}}^\ell\}_{\ell=1}^L, M \right) \\ &= \left\{ f_\theta \left| \begin{array}{l} f_\theta(\mathbf{x}) = \mathbf{c}_{L+1}^\top \text{vec}(\mathcal{T}_L(\mathbf{x})) \text{ is an } L\text{-block Transformer with embedding dim } D, \\ \text{sequence length } P, \text{ parameter bound } \|\theta\|_\infty \leq M, \text{ and for each block } \ell \in [L] : \\ \text{there is } H^\ell \text{ heads, query/key dim is } d_k^\ell, \text{ value dim is } d_v^\ell, \text{ FFN hidden width is } d_{\text{ff}}^\ell \end{array} \right. \right\}. \end{aligned}$$

3 Learning on Euclidean domains

In this section, we establish the theoretical capabilities of the Transformer architecture. We focus our analysis on compact Euclidean domains and introduce a novel Softmax POU framework. In Subsection 3.1, we constructively prove uniform approximation rates for Hölder continuous functions. Building upon these approximation results, we further establish the corresponding statistical generalization bounds in Subsection 3.2.

3.1 Approximation of Hölder functions on Euclidean domains

A foundational ingredient in our construction is the Softmax POU. Unlike deep ReLU networks that rely on locally compactly supported bump functions as POU [45, 46, 32], we introduce a globally supported "soft" POU by Softmax POU. This idea shares connections with classical non-parametric techniques, such as Shepard's method for spatial interpolation [34] and normalized Radial Basis Function (RBF) networks [28]. By utilizing a scaling parameter M_g to control the exponential decay outside local neighborhoods, this scheme naturally establishes a local-to-global approximation paradigm. We formalize this mathematical construction in the following lemma, which is proved in Appendix A.1.

Lemma 1 (Softmax POU Approximation on Euclidean Space). *Let $d \in \mathbb{N}$, $\alpha \in (0, 1]$, and $g : [0, 1]^d \rightarrow \mathbb{R}$ be an α -Hölder continuous function with constant C_H . For any target accuracy $\varepsilon \in (0, \frac{1}{e}]$, let the covering radius be $r_g = (\varepsilon / (4C_H))^{1/\alpha}$. There exists a finite set of C_g centers $\{\mathbf{c}_i\}_{i=1}^{C_g} \subset [0, 1]^d$ forming an r_g -covering of the domain (i.e., $[0, 1]^d \subseteq \bigcup_{i=1}^{C_g} \bar{\mathcal{B}}(\mathbf{c}_i, r_g)$) with*

$C_g \leq \left(\sqrt{d}(4C_H)^{1/\alpha}\right)^d \varepsilon^{-\frac{d}{\alpha}}$. By setting the scaling parameter

$$M_g = \frac{(4C_H)^{2/\alpha}}{3} \left(\log \left(4\|g\|_\infty \left(\sqrt{d}(4C_H)^{1/\alpha}\right)^d \right) + \frac{d+\alpha}{\alpha} \right) \varepsilon^{-\frac{2}{\alpha}} \log \frac{1}{\varepsilon},$$

the Softmax POU approximation $\widehat{g}(\mathbf{x}) = \sum_{i=1}^{C_g} \beta_i(\mathbf{x})g(\mathbf{c}_i)$, with

$$\beta_i(\mathbf{x}) = \frac{\exp(M_g(r_g^2 - \|\mathbf{x} - \mathbf{c}_i\|_2^2))}{\sum_{k=1}^{C_g} \exp(M_g(r_g^2 - \|\mathbf{x} - \mathbf{c}_k\|_2^2))} = \frac{\exp(2M_g \langle \mathbf{x}, \mathbf{c}_i \rangle - M_g\|\mathbf{c}_i\|_2^2)}{\sum_{k=1}^{C_g} \exp(2M_g \langle \mathbf{x}, \mathbf{c}_k \rangle - M_g\|\mathbf{c}_k\|_2^2)}, \quad (3)$$

achieves the uniform error bound $\sup_{\mathbf{x} \in [0,1]^d} |\widehat{g}(\mathbf{x}) - g(\mathbf{x})| \leq \varepsilon$.

Lemma 1 introduces our new approximation framework. The centers $\{\mathbf{c}_i\}_{i=1}^{C_g}$ and the corresponding covering balls $\widehat{\mathcal{B}}(\mathbf{c}_i, r_g)$ induce localized soft regions through the weights $\beta_i(\mathbf{x})$, which is illustrated in Figure 1. The weight functions $\{\beta_i(\mathbf{x})\}_{i=1}^{C_g}$ form a partition of unity over the domain, and the scaling parameter M_g controls the exponential decay of $\beta_i(\mathbf{x})$.

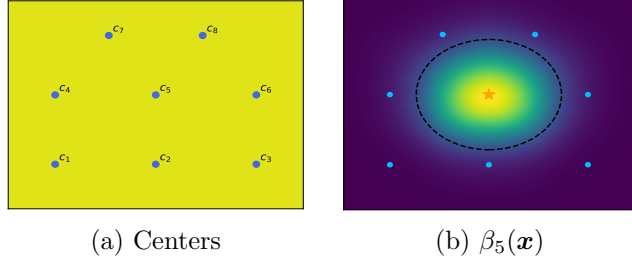


Figure 1: Geometric illustration of the softmax partition of unity. The centers $\{\mathbf{c}_i\}_{i=1}^{C_g}$ and covering balls $\widehat{\mathcal{B}}(\mathbf{c}_i, r_g)$ induce the localized soft weights $\beta_i(\mathbf{x})$.

The Softmax POU approximation scheme offers two primary advantages: (i) the algebraic cancellation of the input-dependent quadratic term $\|\mathbf{x}\|_2^2$ eliminates the geometric quadratic form, reducing the relative distance computation to purely affine transformations; and (ii) it perfectly aligns with the native Transformer architecture, enabling mesh-free spatial localization that is dynamically achieved through standard softmax dot-product attention mechanism. The following theorem quantifies the approximation power of Transformers using the Softmax POU approximation framework.

Theorem 1 (Transformer Approximation on Euclidean Space). *Let $d \in \mathbb{N}$, $\alpha \in (0, 1]$, and $g : [0, 1]^d \rightarrow \mathbb{R}$ be α -Hölder continuous with constant C_H and $\|g\|_\infty \leq B$. For any $\varepsilon \in (0, 1/e]$, there exists a Transformer network*

$$\widehat{g}_T \in \mathcal{T}\left(L, D, P, \{H^\ell\}_{\ell=1}^L, \{d_k^\ell\}_{\ell=1}^L, \{d_v^\ell\}_{\ell=1}^L, \{d_{ff}^\ell\}_{\ell=1}^L, M_{max}\right)$$

satisfying

$$\sup_{\mathbf{x} \in [0,1]^d} |\widehat{g}_T(\mathbf{x}) - g(\mathbf{x})| \leq \varepsilon$$

with the following parameters

- $L = 2$, $D = d + 4$, and $P \leq C_P \varepsilon^{-d/\alpha}$ where $C_P = d^{d/2}(8C_H)^{d/\alpha}$.
- For $\ell = 1$: $H^1 = P + 2$, $d_k^1 = d_v^1 = 2$, and $d_{ff}^1 = 2d + 8$.
- For $\ell = 2$: $H^2 = 1$, $d_k^2 = d_v^2 = 1$, and $d_{ff}^2 = 2d + 8$.

The parameter magnitude M_{max} and total dense parameters \mathcal{N}_{total} satisfy

$$M_{max} \leq \tilde{C}_{mag} \varepsilon^{-2d/\alpha} \log \frac{1}{\varepsilon}, \quad \mathcal{N}_{total} \leq C_N \varepsilon^{-d/\alpha},$$

where $C_N = 10(d+4)C_P + 9d^2 + 95d + 236$, and $\tilde{C}_{mag} = \max \left\{ \frac{1}{1-\frac{1}{eB}}, C_{mag}, 2 \left(1 + \frac{1}{2eB}\right) C_B \right\}$, with $C_B = \max\{3dC_M, B, 1\}$, $C_{mag} = \frac{C_P^2 C_{log}}{8}$, $C_{log} = |\log(4C_P B(1+6dC_M))| + \frac{d+2+\alpha}{\alpha} + 2$, and $C_M = \frac{(8C_H)^{2/\alpha}}{3} (\log(4Bd^{d/2}(4C_H)^{d/\alpha}) + \frac{d+\alpha}{\alpha})$.

The constructive approximation established in Theorem 1 reveals several architectural alignments between our theoretical framework and practical Transformer implementations:

- **Shallow, Wide, and Dense Architecture:** Our framework achieves the desired approximation accuracy with remarkably shallow ($L = 2$), wide, and dense Transformers equipped with standard single-hidden-layer pointwise FFNs. Instead of relying on increased network depth, the model’s representational capacity is primarily concentrated in the sequence dimension P . This architecture enables extensive feature interactions while maintaining a low compositional depth, which is particularly well-suited for parallel computation.
- **Native Softmax Attention Mechanism:** By strictly utilizing the standard dot-product attention and softmax activation, we prove that practical attention mechanisms natively achieve precise spatial localization, completely avoiding contrived mathematical activations.
- **Sinusoidal Positional Encodings:** Rather than employing artificial spatial embeddings, our framework utilizes standard sinusoidal encodings defined on a uniform angular grid. We demonstrate that this angular geometry natively computes relative positions via phase differences, and exploits exact cyclic symmetries to ensure that the angular identity of each token remains invariant across layers.

Proof Sketch of Theorem 1. The detailed proof of Theorem 1 is deferred to Appendix B.1. We construct a 2-block Transformer to execute the Softmax POU approximation scheme by leveraging the sequence dimension P as an index set to parallelize the localized expert approximations. The procedure is organized into four key stages:

Pre-processing (see Lemma 4): The input $\mathbf{x} \in [0, 1]^d$ is mapped to an initial sequence matrix $\mathbf{Z}_0 \in \mathbb{R}^{D \times P}$. This layer embeds \mathbf{x} and an indicator exclusively into the first token, zero-pads the remaining sequence, and appends sinusoidal positional encodings across all P tokens

$$(\mathbf{Z}_0)_{:,j} = [\delta_{j,1} \mathbf{x}^\top, \delta_{j,1}, 0, \sin(\theta_j), \cos(\theta_j)]^\top.$$

First MHA (Local Feature Extraction, see Lemma 5): Utilizing $H^1 = P + 2$ heads, this layer computes parallel affine transformations to extract local spatial features and approximation expert features. The output $\hat{\mathbf{Z}}_1 = \mathcal{A}_1(\mathbf{Z}_0)$ takes the column-wise form

$$(\hat{\mathbf{Z}}_1)_{:,j} = \left[\tilde{T}_j(\mathbf{x}), \tilde{g}(\mathbf{c}_j), \mathbf{0}_{d-1}^\top, \tilde{I}_j, \lambda(M) \sin(\theta_j), \lambda(M) \cos(\theta_j) \right]^\top,$$

where $\tilde{T}_j(\mathbf{x}) \approx 2M_g \mathbf{c}_j^\top \mathbf{x} - M_g \|\mathbf{c}_j\|_2^2$ captures the approximated local spatial feature, $\tilde{g}(\mathbf{c}_j) \approx g(\mathbf{c}_j)$ represents the approximated local expert feature for each center \mathbf{c}_j , and $\tilde{I}_j \approx \delta_{j,1}$ serves as the

approximated structural indicator for the first token. Crucially, in our construction, the exact angular identity θ_j of the sinusoidal positional encodings remains invariant up to a uniform scalar scaling $\lambda(M)$.

First FFN (Non-linear Restoration, see Lemma 6): By exploiting the hard-thresholding gating property of the ReLU activation, $\mathbf{Z}_1 = \mathcal{F}_1(\widehat{\mathbf{Z}}_1)$ functions as a non-linear filter to eliminate the small error introduced by the softmax operation, thereby exactly recovering the canonical form and original sinusoidal positional encodings

$$(\mathbf{Z}_1)_{:,j} = \left[\widetilde{T}_j(\mathbf{x}), \widetilde{g}(\mathbf{c}_j), \mathbf{0}_{d-1}^\top, \delta_{j,1}, \sin(\theta_j), \cos(\theta_j) \right]^\top.$$

Second MHA (Global Aggregation, see Lemma 7): A single head ($H^2 = 1$) extracts the indicator $\delta_{k,1}$ via the Query, the local spatial features $\widetilde{T}_j(\mathbf{x})$ via the Key, and the local expert features $\widetilde{g}(\mathbf{c}_j)$ via the Value. The softmax activation then directly computes the normalized POU weights $\beta_j(\mathbf{x}) = \exp(\widetilde{T}_j(\mathbf{x})) / \sum_{l=1}^P \exp(\widetilde{T}_l(\mathbf{x}))$, aggregating the local expert predictions into a unified global approximation $\widehat{g}_T(\mathbf{x})$ and storing the result in the first column of $\widehat{\mathbf{Z}}_2 = \mathcal{A}_2(\mathbf{Z}_1)$, that is

$$(\widehat{\mathbf{Z}}_2)_{:,1} = \left[\widehat{g}_T(\mathbf{x}), \mathbf{0}_{D-1}^\top \right]^\top, \quad \text{where} \quad \widehat{g}_T(\mathbf{x}) = \sum_{j=1}^P \beta_j(\mathbf{x}) \widetilde{g}(\mathbf{c}_j).$$

Second FFN & Readout: Finally, \mathcal{F}_2 operates as an exact identity mapping $\mathbf{Z}_2 = \widehat{\mathbf{Z}}_2$. A linear readout vector \mathbf{c}^\top explicitly extracts the final approximation $\widehat{g}_T(\mathbf{x})$ from the hidden state. \square

3.2 Generalization analysis

In this section, we analyze the generalization capability of the empirical risk minimization (ERM) algorithm over the bounded hypothesis space constructed based on our Transformer architecture. We utilize the covering number to measure the capacity of the hypothesis space, which subsequently provides insights into the learning performance of the ERM algorithm.

We follow the classical learning framework for regression [7]. Suppose that a data sample $\mathcal{S} = \{(\mathbf{x}_i, y_i)\}_{i=1}^n \subset \mathcal{X} \times \mathcal{Y}$ is independently drawn from a true unknown Borel probability measure ρ on $\mathcal{X} \times \mathcal{Y}$, with $\mathcal{Y} \subseteq [-B, B]$ for some $B > 0$. The target function for learning is the regression function $f_\rho : \mathcal{X} \rightarrow \mathbb{R}$ defined by $f_\rho(\mathbf{x}) = \int_{\mathcal{Y}} y d\rho(y|\mathbf{x})$, which minimizes the expected generalization error

$$\mathcal{E}(f) := \int_{\mathcal{X} \times \mathcal{Y}} (f(\mathbf{x}) - y)^2 d\rho.$$

We denote by $\rho_{\mathcal{X}}$ the marginal distribution of ρ on \mathcal{X} , and by $(L_{\rho_{\mathcal{X}}}^2, \|\cdot\|_\rho)$ the Hilbert space of square-integrable functions with respect to $\rho_{\mathcal{X}}$.

We consider the ERM algorithm over the Transformer hypothesis space \mathcal{T} defined in Theorem 1. Based on this hypothesis space, the ERM algorithm learns the empirical target function

$$f_{\mathcal{S}} := \arg \min_{f \in \mathcal{T}} \frac{1}{n} \sum_{i=1}^n (f(\mathbf{x}_i) - y_i)^2.$$

Since $\mathcal{Y} \subseteq [-B, B]$, we project the output function onto the interval $[-B, B]$ and define the truncated empirical target function as $\pi_B f_{\mathcal{S}}$, where $\pi_B(t) = \max\{-B, \min\{t, B\}\}$.

For target functions defined on Euclidean domains, based on the approximation error bound in

Theorem 1 and the covering number bound in Lemma 9 in Appendix C.1, we obtain the following near minimax-optimal convergence rate of the Transformer estimator f_S .

Theorem 2. *Suppose that the regression function $f_\rho : [0, 1]^d \rightarrow \mathbb{R}$ is an α -Hölder continuous function with constant C_H and $\|f_\rho\|_\infty \leq B$. Consider the truncated empirical target function $\pi_B f_S$ over the hypothesis space \mathcal{T} defined in Theorem 1, for $0 < \varepsilon \leq 1/e$, we have*

$$\mathbb{E} \left[\|\pi_B f_S - f_\rho\|_\rho^2 \right] \leq C_4 \max \left\{ \varepsilon^2, \frac{\varepsilon^{-d/\alpha} \log \frac{1}{\varepsilon}}{n} \right\}.$$

Moreover, by choosing $\varepsilon = n^{-\frac{\alpha}{2\alpha+d}}$, we obtain

$$\mathbb{E} \left[\|\pi_B f_S - f_\rho\|_\rho^2 \right] \leq C_4 n^{-\frac{2\alpha}{2\alpha+d}} \log n,$$

where C_4 is a positive constant depending on d, α, B , and C_H specified in (13).

Proof Sketch of Theorem 2. The detailed proof is deferred to Appendix C. The result follows from optimizing the bias-variance trade-off established via an oracle inequality (Lemma 10). First, we bound the approximation error (bias) by ε utilizing the Transformer construction from Theorem 1. Second, we control the estimation error (variance) by bounding the capacity of the hypothesis space \mathcal{T} as detailed in Appendix Subsection C.1. Specifically, Lemma 9 provides the covering number bound

$$\log \mathcal{N}(\eta, \mathcal{T}, \|\cdot\|_\infty) \leq \mathcal{N}_{total} \log \left(\frac{1224256P^4 D^{22} M_{max}^{26}}{\eta} \right).$$

Finally, balancing the approximation and estimation errors and choosing the optimal network accuracy $\varepsilon = n^{-\frac{\alpha}{2\alpha+d}}$ yields the desired convergence rate as detailed in Appendix Subsection C.2. \square

4 Adaptivity to Riemannian manifolds

In this section, we assume that the input domain $\mathcal{M} \subseteq [0, 1]^{\bar{d}}$ is a compact and connected d -dimensional Riemannian manifold with strictly positive reach $\tau > 0$ (see Definition 2 in Appendix A.2). Our goal is to investigate the theoretical capabilities of Transformers for learning α -Hölder continuous functions defined on \mathcal{M} (see Definition 3 in Appendix A.2). More details about manifolds can be found in [42, 23].

Our Softmax POU approximation scheme naturally adapts to complex geometries by operating directly on the ambient Euclidean metric. Because the ReLU activation is fundamentally piecewise linear, locally supported ReLU-based POUs are geometrically constrained to partition space using hyperplanes, such as explicit Cartesian grids or simplicial triangulations. In contrast, the Softmax POU is inherently mesh-free. By exploiting the local metric equivalence between intrinsic geodesic and ambient Euclidean distances, it achieves spatial localization purely through affine transformations, avoiding the need for explicit surface parameterizations or complex non-linear geodesic computations. This exact formulation perfectly aligns with the native dot-product attention mechanism in Transformers. Building upon this geometric intuition, the following theorem formally establishes how Transformers natively execute this local-to-global approximation scheme to bypass the geometric complexities of compact Riemannian manifolds.

Theorem 3 (Transformer Approximation on Manifolds). *Let $\mathcal{M} \subseteq [0, 1]^{\bar{d}}$ be a d -dimensional compact and connected Riemannian manifold with reach $\tau > 0$, and let $g : \mathcal{M} \rightarrow \mathbb{R}$ be an α -Hölder continuous function with constant C_H and $\|g\|_\infty \leq B$. For any ε satisfying $0 < \varepsilon \leq \min \left\{ \frac{1}{e}, 16C_H \left(\frac{\tau}{4} \right)^\alpha \right\}$, there exists a Transformer network*

$$\hat{g}_T \in \mathcal{T} \left(L, \bar{d} + 4, P, \{H^\ell\}_{\ell=1}^L, \{d_k^\ell\}_{\ell=1}^L, \{d_v^\ell\}_{\ell=1}^L, \{d_{ff}^\ell\}_{\ell=1}^L, M_{max} \right)$$

satisfying

$$\sup_{\mathbf{x} \in \mathcal{M}} |\hat{g}_T(\mathbf{x}) - g(\mathbf{x})| \leq \varepsilon$$

with the following parameters:

- $L = 2$, embedding dimension $D = \bar{d} + 4$, and $P \leq C_P \varepsilon^{-d/\alpha}$ where $C_P = C_{\mathcal{M}}(16C_H)^{d/\alpha}$.
- For $\ell = 1$: $H^1 = P + 2$, $d_k^1 = d_v^1 = 2$, and $d_{ff}^1 = 2\bar{d} + 8$.
- For $\ell = 2$: $H^2 = 1$, $d_k^2 = d_v^2 = 1$, and $d_{ff}^2 = 2\bar{d} + 8$.

The parameter magnitude M_{max} and total dense parameters \mathcal{N}_{total} satisfy

$$M_{max} \leq \tilde{C}_{mag} \varepsilon^{-2d/\alpha} \log \frac{1}{\varepsilon}, \quad \mathcal{N}_{total} \leq C_N \varepsilon^{-d/\alpha},$$

where $C_N = 10(\bar{d} + 4)C_P + 9\bar{d}^2 + 95\bar{d} + 236$, $\tilde{C}_{mag} = \max \left\{ \frac{1}{1 - \frac{1}{eB}}, C_{mag}, 2 \left(1 + \frac{1}{2eB} \right) C_B \right\}$, with $C_B = \max\{3\bar{d}C_M, B, 1\}$, $C_{mag} = \frac{C_P^2 C_{log}}{8}$, $C_{log} = |\log(2C_P B(1 + 6\bar{d}C_M))| + \frac{d+2+\alpha}{\alpha} + 2$, $C_M = \frac{(16C_H)^{2/\alpha}}{3} (\log(4BC_P) + \frac{d+\alpha}{\alpha})$, $C_{\mathcal{M}} = 3^d \text{Vol}(\mathcal{M})d^{d/2}$, and $\text{Vol}(\mathcal{M})$ is the volume of \mathcal{M} .

The rigorous establishment of this approximation guarantee relies on several key geometric tools detailed in Appendix A.2. Specifically, we leverage the local metric equivalence between the geodesic and Euclidean distances governed by the reach τ , alongside the intrinsic covering number bounds of manifolds (see Lemma 2). These geometric properties theoretically validate the extension of our Softmax POU scheme to the manifold setting (see Lemma 3). The detailed proof of Theorem 3 is deferred to Appendix B.2. The architectural construction follows a similar procedure to the proof of Theorem 1, but adapts the scaling factor and sequence length to the covering properties of \mathcal{M} . Based on this approximation theorem, we further establish the statistical convergence rate of the Transformer estimator f_S for target functions defined on manifolds.

Theorem 4. *Suppose that the regression function $f_\rho : \mathcal{M} \rightarrow \mathbb{R}$ is an α -Hölder continuous function with constant C_H and $\|f_\rho\|_\infty \leq B$, where $\mathcal{M} \subseteq [0, 1]^{\bar{d}}$ is a compact and connected d -dimensional Riemannian manifold with reach $\tau > 0$. Consider the truncated empirical target function $\pi_B f_S$ over the hypothesis space \mathcal{T} defined in Theorem 3, for $0 < \varepsilon \leq \min \left\{ \frac{1}{e}, 16C_H \left(\frac{\tau}{4} \right)^\alpha \right\}$, we have*

$$\mathbb{E} \left[\|\pi_B f_S - f_\rho\|_\rho^2 \right] \leq \tilde{C}_4 \max \left\{ \varepsilon^2, \frac{\varepsilon^{-d/\alpha} \log \frac{1}{\varepsilon}}{n} \right\}.$$

Moreover, by choosing $\varepsilon = n^{-\frac{\alpha}{2\alpha+d}}$, we obtain

$$\mathbb{E} \left[\|\pi_B f_S - f_\rho\|_\rho^2 \right] \leq \tilde{C}_4 n^{-\frac{2\alpha}{2\alpha+d}} \log n,$$

Table 1: Comparison of Transformer architectures between our work and existing theories.

References	Softmax Attention	Sinusoidal PE	Depth
Gurevych et al. [17]	✗	✗	$\mathcal{O}(1)$
Takakura and Suzuki [41]	✓	✓	$\mathcal{O}(\text{poly}(\log(1/\varepsilon)))$
Havrilla and Liao [18]	✗	✓	$\mathcal{O}(\log(1/\varepsilon))$
Shi et al. [36]	✓	✗	$\mathcal{O}(\log(1/\varepsilon))$
Jiao et al. [20]	✓	✗	$\mathcal{O}(\log(1/\varepsilon))$
Ours (This work)	✓	✓	2

where \tilde{C}_4 is a positive constant depending on $\bar{d}, d, \alpha, B, C_H$, and $\text{Vol}(\mathcal{M})$ specified in (14).

The detailed proof of Theorem 4 is deferred to Appendix C. Similar to the Euclidean setting, Theorem 4 is derived by utilizing the bias-variance tradeoff and the covering number bound of the Transformer hypothesis space. Crucially, notice that the final learning rate depends exclusively on the intrinsic dimension d rather than the ambient dimension \bar{d} . This demonstrates that our shallow, wide, and dense Transformer architecture can effectively avoid the curse of dimensionality when processing data intrinsically supported on low-dimensional manifolds.

5 Related work and discussion

In this section, we discuss existing works that are closely related to this paper.

Learning Theory of Transformers. Recent studies have investigated the quantitative approximation and estimation capabilities of Transformers [17, 41, 19, 18, 36, 20]. Specifically, they show that Transformers can circumvent this curse when target functions exhibit hierarchical compositional structures [17, 36] or anisotropic smoothness in sequence-to-sequence tasks [41]. Further research has established Jackson-type rates demonstrating their theoretical superiority over RNNs [19], and utilized the Kolmogorov-Arnold theorem for Hölder function approximation [20]. However, prior studies often rely on mathematical contrivances, such as hardmax attention, canonical positional encodings, or excessive network depth, that diverge from practical implementations. For instance, to bypass the excessive depth typically required to approximate non-linear multiplications, [17, 18] substitute the standard softmax with hardmax and ReLU attention mechanisms, respectively. These modified activations naturally generate multiplications, which significantly simplifies the polynomial approximation problem and therefore allows network depth to $\mathcal{O}(1)$. In contrast, our framework reveals the potential of Transformers by exploiting the native softmax attention mechanism and sinusoidal positional encodings within a shallow architecture ($L = 2$). Note that throughout our comparisons, the overall Transformer network depth is evaluated as the sum of the depths of the internal point-wise FFNs across all encoder blocks. A detailed comparison with previous work is summarized in Table 1.

Learning Theory on Manifolds. To mitigate the curse of dimensionality, extensive research has shown that neural network architectures, including deep ReLU FFNs [3, 4], CNNs [24], autoencoders [25], and Transformers [18], can adapt to the intrinsic low-dimensional geometry of data. These studies demonstrate that for functions on manifolds, network complexity and generalization bounds scale with the intrinsic dimension and can overcome the curse of dimensionality [3, 29, 24, 6, 4, 8, 25]. However, these approximation schemes fundamentally rely on

deep ReLU structures and inherently require $\mathcal{O}(\log(1/\varepsilon))$ depth to achieve high precision. In contrast, our construction demonstrates that shallow, wide, and dense Transformers can attain near minimax-optimal learning rates on manifolds, completely bypassing the need for structural depth dependencies or artificial sparsity constraints.

6 Conclusion

In this paper, we establish a novel local-to-global constructive approximation framework for Transformers based on a globally supported Softmax POU. Leveraging this framework, we provide comprehensive approximation and generalization guarantees for α -Hölder continuous functions on both compact Euclidean domains and Riemannian manifolds, where we restrict $\alpha \in (0, 1]$. Specifically, we prove that shallow, wide, and dense Transformers with softmax activation and sinusoidal positional encodings can attain near minimax-optimal convergence rates and overcome the curse of dimensionality. A compelling future direction is to explore the potential of our Softmax POU framework for analyzing the mechanisms of in-context learning [2, 9, 33]. While classic studies often interpret this phenomenon by viewing Transformers as implicit statisticians [1] or as executing internal learning algorithms [13], our constructive scheme offers a potentially distinct perspective to further investigate how Transformer architectures achieve adaptive approximations during inference.

Appendix

This appendix provides the complete mathematical proofs for our theoretical results. It is organized as follows: Section A proves the preliminary lemmas for the Softmax POU scheme and Transformer constructions; Section B establishes the main approximation guarantees for both Euclidean domains and Riemannian manifolds; and Section C details the covering number bounds and the derivation of the generalization error rates.

A Proof of preliminary results

This section establishes the detailed proofs for the foundational mathematical tools used in our theoretical framework. We first prove the Softmax POU approximation schemes and then provide the constructive lemmas for individual Transformer layers.

A.1 Softmax POU scheme for Euclidean domains in Section 3

In this subsection, we present the proof of Lemma 1. This establishes the core mechanism of using a Softmax POU to achieve local-to-global approximation on compact Euclidean spaces.

Proof of Lemma 1. To construct the approximation, we first explicitly establish the finite covering and bound the required number of centers C_g . For any target accuracy $\varepsilon \in (0, 1/e]$, we set the covering radius as $r_g = (\varepsilon/(4C_H))^{1/\alpha}$. We partition the domain $[0, 1]^d$ into a uniform grid of hypercubes. By strategically setting the side length of each hypercube to $\delta = 2r_g/\sqrt{d}$, the distance from its center to any vertex (i.e., the circumscribed radius) is exactly $\frac{1}{2}\sqrt{d}\delta^2 = r_g$. This guarantees that a closed Euclidean ball $\bar{\mathcal{B}}(\mathbf{c}_k, r_g)$ centered at the midpoint \mathbf{c}_k of each hypercube completely covers it, yielding a valid finite cover of $[0, 1]^d$.

The number of grid points required along each dimension is exactly $\lceil 1/\delta \rceil$, resulting in a total of $C_g = \lceil 1/\delta \rceil^d$ centers. By the inequality that $\lceil x \rceil \leq 2x$ when $x \geq 1$, we have

$$C_g = \left\lceil \frac{1}{\delta} \right\rceil^d = \left\lceil \frac{\sqrt{d}}{2r_g} \right\rceil^d \leq \left(2 \cdot \frac{\sqrt{d}}{2r_g} \right)^d = \left(\frac{\sqrt{d}}{r_g} \right)^d = \left(\sqrt{d}(4C_H)^{1/\alpha} \right)^d \varepsilon^{-\frac{d}{\alpha}}.$$

With the centers $\{\mathbf{c}_i\}_{i=1}^{C_g}$ and the covering established, for any $\mathbf{x} \in [0, 1]^d$, denote $i^*(\mathbf{x}) = \operatorname{argmin}_{i \in [C_g]} \|\mathbf{x} - \mathbf{c}_i\|_2$. Since the closed balls cover the domain, we are guaranteed that $\|\mathbf{x} - \mathbf{c}_{i^*}\|_2 \leq r_g$.

Next, we bound the approximation error. Notice that $\beta_i(\mathbf{x}) = \frac{\exp(M_g(r_g^2 - \|\mathbf{x} - \mathbf{c}_i\|_2^2))}{\sum_{k=1}^{C_g} \exp(M_g(r_g^2 - \|\mathbf{x} - \mathbf{c}_k\|_2^2))}$, using the exact POU property that $\sum_{i=1}^{C_g} \beta_i(\mathbf{x}) = 1$, we decompose the error into near and far components at a radius of $2r_g$, that is

$$\begin{aligned} |\widehat{g}(\mathbf{x}) - g(\mathbf{x})| &= \left| \sum_{i=1}^{C_g} \beta_i(\mathbf{x})(g(\mathbf{c}_i) - g(\mathbf{x})) \right| \\ &\leq \underbrace{\sum_{i: \|\mathbf{x} - \mathbf{c}_i\|_2 \leq 2r_g} \beta_i(\mathbf{x}) |g(\mathbf{x}) - g(\mathbf{c}_i)|}_{(I)} + \underbrace{\sum_{i: \|\mathbf{x} - \mathbf{c}_i\|_2 > 2r_g} \beta_i(\mathbf{x}) |g(\mathbf{x}) - g(\mathbf{c}_i)|}_{(II)}. \end{aligned}$$

For the near-center terms (I), the α -Hölder continuity yields $|g(\mathbf{x}) - g(\mathbf{c}_i)| \leq C_H(2r_g)^\alpha \leq 2C_H r_g^\alpha$ since $2^\alpha \leq 2$ for $\alpha \in (0, 1]$. By substituting our explicit choice of r_g , we obtain

$$(I) \leq 2C_H r_g^\alpha \sum_i \beta_i(\mathbf{x}) \leq 2C_H r_g^\alpha = 2C_H \left(\frac{\varepsilon}{4C_H} \right) = \frac{\varepsilon}{2}.$$

For the far-center tail terms (II), the condition $\|\mathbf{x} - \mathbf{c}_i\|_2 > 2r_g$ implies $r_g^2 - \|\mathbf{x} - \mathbf{c}_i\|_2^2 < -3r_g^2$. Since $\|\mathbf{x} - \mathbf{c}_{i^*}\|_2 \leq r_g$, the denominator of $\beta_i(\mathbf{x})$ is bounded below

$$\sum_{k=1}^{C_g} \exp(M_g(r_g^2 - \|\mathbf{x} - \mathbf{c}_k\|_2^2)) \geq \exp(M_g(r_g^2 - \|\mathbf{x} - \mathbf{c}_{i^*}\|_2^2)) \geq \exp(0) = 1.$$

Applying the global bound $|g(\mathbf{x}) - g(\mathbf{c}_i)| \leq 2\|g\|_\infty$, the term (II) is bounded by

$$\begin{aligned} (II) &= \sum_{i: \|\mathbf{x} - \mathbf{c}_i\|_2 > 2r_g} \frac{\exp(M_g(r_g^2 - \|\mathbf{x} - \mathbf{c}_i\|_2^2))}{\sum_{k=1}^{C_g} \exp(M_g(r_g^2 - \|\mathbf{x} - \mathbf{c}_k\|_2^2))} |g(\mathbf{x}) - g(\mathbf{c}_i)| \\ &\leq \sum_{i: \|\mathbf{x} - \mathbf{c}_i\|_2 > 2r_g} \exp(-3M_g r_g^2) \cdot 2\|g\|_\infty \\ &\leq 2C_g \|g\|_\infty \exp(-3M_g r_g^2). \end{aligned}$$

To guarantee (II) $\leq \varepsilon/2$, the scaling parameter must satisfy $M_g \geq (3r_g^2)^{-1} \log(4C_g \|g\|_\infty / \varepsilon)$.

Substituting the explicit formulas for r_g and C_g , we require

$$\begin{aligned} M_g &\geq \frac{(4C_H)^{2/\alpha}}{3} \varepsilon^{-\frac{2}{\alpha}} \log \left(4\|g\|_\infty \left(\sqrt{d}(4C_H)^{1/\alpha} \right)^d \varepsilon^{-\frac{d+\alpha}{\alpha}} \right) \\ &= \frac{(4C_H)^{2/\alpha}}{3} \varepsilon^{-\frac{2}{\alpha}} \left(\log \left(4\|g\|_\infty \left(\sqrt{d}(4C_H)^{1/\alpha} \right)^d \right) + \frac{d+\alpha}{\alpha} \log \frac{1}{\varepsilon} \right). \end{aligned}$$

Assuming $\varepsilon \leq 1/e$ so that $\log(1/\varepsilon) \geq 1$, we can upper bound the bracketed sum by factoring out $\log(1/\varepsilon)$. Defining M_g as

$$M_g = \frac{(4C_H)^{2/\alpha}}{3} \left(\log \left(4\|g\|_\infty \left(\sqrt{d}(4C_H)^{1/\alpha} \right)^d \right) + \frac{d+\alpha}{\alpha} \right) \varepsilon^{-\frac{2}{\alpha}} \log \frac{1}{\varepsilon}$$

satisfies this condition, ensuring $(II) \leq \varepsilon/2$.

Combining (I) and (II) achieves the target uniform error

$$\sup_{\mathbf{x} \in [0,1]^d} |\widehat{g}(\mathbf{x}) - g(\mathbf{x})| \leq \frac{\varepsilon}{2} + \frac{\varepsilon}{2} = \varepsilon.$$

Finally, notice that the quadratic term $\|\mathbf{x}\|_2^2$ exactly cancels out in the Softmax expansion, we have

$$\begin{aligned} \beta_i(\mathbf{x}) &= \frac{\exp(M_g(r_g^2 - \|\mathbf{x}\|_2^2)) \exp(2M_g \langle \mathbf{x}, \mathbf{c}_i \rangle - M_g \|\mathbf{c}_i\|_2^2)}{\sum_{k=1}^{C_g} \exp(M_g(r_g^2 - \|\mathbf{x}\|_2^2)) \exp(2M_g \langle \mathbf{x}, \mathbf{c}_k \rangle - M_g \|\mathbf{c}_k\|_2^2)} \\ &= \frac{\exp(2M_g \langle \mathbf{x}, \mathbf{c}_i \rangle - M_g \|\mathbf{c}_i\|_2^2)}{\sum_{k=1}^{C_g} \exp(2M_g \langle \mathbf{x}, \mathbf{c}_k \rangle - M_g \|\mathbf{c}_k\|_2^2)}, \end{aligned}$$

thus we complete the proof. \square

A.2 Softmax POU scheme for manifolds in Section 4

Here, we extend our Softmax POU approximation scheme to compact Riemannian manifolds (See Lemma 3). We leverage the intrinsic geometric properties and local metric equivalence to properly bound the approximation errors. We first introduce some definitions and notations about Riemannian manifolds. Let $d(\mathbf{x}, \mathcal{M}) := \inf_{\mathbf{v} \in \mathcal{M}} \|\mathbf{x} - \mathbf{v}\|_2$ denote the Euclidean distance from a point $\mathbf{x} \in \mathbb{R}^{\bar{d}}$ to a manifold $\mathcal{M} \subset \mathbb{R}^{\bar{d}}$. To characterize the curvature and the folding of \mathcal{M} within the ambient space, we introduce the concept of reach.

Definition 2 (Reach [12, 30]). *The reach of \mathcal{M} is defined as*

$$\tau = \inf_{\mathbf{v} \in \mathcal{M}} \inf_{\mathbf{x} \in G} \|\mathbf{x} - \mathbf{v}\|_2,$$

where $G = \left\{ \mathbf{x} \in \mathbb{R}^{\bar{d}} : \exists \text{ distinct } \mathbf{p}, \mathbf{q} \in \mathcal{M} \text{ such that } d(\mathbf{x}, \mathcal{M}) = \|\mathbf{x} - \mathbf{p}\|_2 = \|\mathbf{x} - \mathbf{q}\|_2 \right\}$ is the medial axis of \mathcal{M} .

We equip the compact and connected Riemannian manifold \mathcal{M} with the intrinsic geodesic metric

$d_{\mathcal{M}} : \mathcal{M} \times \mathcal{M} \rightarrow \mathbb{R}_{\geq 0}$, defined as

$$d_{\mathcal{M}}(\mathbf{x}, \mathbf{y}) := \inf \left\{ \int_0^1 \|\dot{\gamma}(t)\|_2 dt \mid \gamma \in C^1([0, 1], \mathcal{M}), \gamma(0) = \mathbf{x}, \gamma(1) = \mathbf{y} \right\}.$$

Based on this metric space $(\mathcal{M}, d_{\mathcal{M}})$, we define the Hölder continuous functions on the manifolds.

Definition 3 (Hölder Continuous Functions on Manifolds). *Let $\alpha \in (0, 1]$, $(\mathcal{M}, d_{\mathcal{M}})$ be a compact and connected d -dimensional Riemannian manifold. A function $f : \mathcal{M} \rightarrow \mathbb{R}$ is α -Hölder continuous if there exists a constant $C_H \geq 0$ such that*

$$|f(\mathbf{x}) - f(\mathbf{y})| \leq C_H \cdot [d_{\mathcal{M}}(\mathbf{x}, \mathbf{y})]^\alpha, \quad \forall \mathbf{x}, \mathbf{y} \in \mathcal{M}.$$

Recall that the ϵ -covering number $\mathcal{N}(X, \epsilon, d)$ is the minimum number of open balls of radius ϵ needed to cover a metric space (X, d) . Since the Euclidean chordal distance is naturally upper-bounded by the intrinsic geodesic distance (i.e., $\|\mathbf{x} - \mathbf{y}\|_2 \leq d_{\mathcal{M}}(\mathbf{x}, \mathbf{y})$), any valid ϵ -covering under $d_{\mathcal{M}}$ is strictly an ϵ -covering under $\|\cdot\|_2$. This topological inclusion directly yields $\mathcal{N}(\mathcal{M}, \epsilon, \|\cdot\|_2) \leq \mathcal{N}(\mathcal{M}, \epsilon, d_{\mathcal{M}})$. The following lemma establishes the bounds for these covering numbers and the local metric equivalence.

Lemma 2. *Let $\mathcal{M} \subseteq [0, 1]^{\bar{d}}$ be a d -dimensional compact and connected Riemannian manifold with reach $\tau > 0$.*

1. (Metric Equivalence [14, Lemma 3]) *For any $\mathbf{x}, \mathbf{y} \in \mathcal{M}$ such that $\|\mathbf{x} - \mathbf{y}\|_2 \leq \tau/2$, the intrinsic geodesic distance satisfies*

$$d_{\mathcal{M}}(\mathbf{x}, \mathbf{y}) \leq \tau \left(1 - \sqrt{1 - \frac{2\|\mathbf{x} - \mathbf{y}\|_2}{\tau}} \right) \leq 2\|\mathbf{x} - \mathbf{y}\|_2. \quad (4)$$

2. (Covering Number Bound [30]) *For any $0 < \epsilon \leq \tau/2$, the covering numbers of \mathcal{M} are bounded by*

$$\mathcal{N}(\mathcal{M}, \epsilon, \|\cdot\|_2) \leq \mathcal{N}(\mathcal{M}, \epsilon, d_{\mathcal{M}}) \leq C_{\mathcal{M}} \epsilon^{-d}, \quad (5)$$

where $C_{\mathcal{M}} = 3^d \text{Vol}(\mathcal{M}) d^{d/2}$, and $\text{Vol}(\mathcal{M})$ is the volume of \mathcal{M} .

With the local metric equivalence and intrinsic covering number bound of manifolds established, we proceed to the Softmax POU approximation scheme on Riemannian manifolds. The proof controls the near-center error using the intrinsic Hölder continuity, and bounds the far-field error through the exponential decay of the ambient Softmax weights.

Lemma 3 (Softmax POU Approximation on Manifolds). *Let $\mathcal{M} \subseteq [0, 1]^{\bar{d}}$ be a compact and connected d -dimensional Riemannian manifold with reach $\tau > 0$, and let $g : \mathcal{M} \rightarrow \mathbb{R}$ be an α -Hölder continuous function with constant C_H . For any target accuracy ϵ satisfying $0 < \epsilon \leq \min \left\{ \frac{1}{e}, 8C_H \left(\frac{\tau}{4} \right)^\alpha \right\}$, let the covering radius be $r_g = (\epsilon / (8C_H))^{1/\alpha}$. There exists a finite set of C_g centers $\{\mathbf{c}_i\}_{i=1}^{C_g} \subset \mathcal{M}$ forming an open r_g -covering of the manifold (i.e., $\mathcal{M} \subseteq \bigcup_{i=1}^{C_g} \mathcal{B}(\mathbf{c}_i, r_g)$) with $C_g \leq C_{\mathcal{M}} (8C_H)^{d/\alpha} \epsilon^{-d/\alpha}$. By setting the scaling parameter*

$$M_g = C_M \epsilon^{-2/\alpha} \log \frac{1}{\epsilon}, \quad \text{where } C_M = \frac{(8C_H)^{2/\alpha}}{3} \left(\log \left(4\|g\|_\infty C_{\mathcal{M}} (8C_H)^{d/\alpha} \right) + \frac{d + \alpha}{\alpha} \right),$$

the ambient Softmax POU approximation

$$\widehat{g}(\mathbf{x}) = \sum_{i=1}^{C_g} \beta_i(\mathbf{x}) g(\mathbf{c}_i),$$

with

$$\beta_i(\mathbf{x}) = \frac{\exp(M_g(r_g^2 - \|\mathbf{x} - \mathbf{c}_i\|_2^2))}{\sum_{k=1}^{C_g} \exp(M_g(r_g^2 - \|\mathbf{x} - \mathbf{c}_k\|_2^2))} = \frac{\exp(2M_g \langle \mathbf{x}, \mathbf{c}_i \rangle - M_g \|\mathbf{c}_i\|_2^2)}{\sum_{k=1}^{C_g} \exp(2M_g \langle \mathbf{x}, \mathbf{c}_k \rangle - M_g \|\mathbf{c}_k\|_2^2)}, \quad (6)$$

achieves the uniform approximation bound

$$\sup_{\mathbf{x} \in \mathcal{M}} |\widehat{g}(\mathbf{x}) - g(\mathbf{x})| \leq \varepsilon.$$

Proof of Lemma 3. To construct the approximation, we first establish a finite covering of the data manifold \mathcal{M} by open Euclidean balls $\{\mathcal{B}(\mathbf{c}_i, r_g)\}_{i=1}^{C_g}$ of radius $r_g > 0$, with centers $\mathbf{c}_i \in \mathcal{M}$. By the covering number bound in Lemma 2, such an open covering exists with the number of centers bounded by $C_g \leq C_{\mathcal{M}} r_g^{-d}$. For any $\mathbf{x} \in \mathcal{M}$, let $i^*(\mathbf{x}) = \operatorname{argmin}_{i \in [C_g]} \|\mathbf{x} - \mathbf{c}_i\|_2$. Since these open balls cover \mathcal{M} , we are guaranteed that $\|\mathbf{x} - \mathbf{c}_{i^*}\|_2 < r_g$. Notice that $\beta_i(\mathbf{x}) = \frac{\exp(M_g(r_g^2 - \|\mathbf{x} - \mathbf{c}_i\|_2^2))}{\sum_{k=1}^{C_g} \exp(M_g(r_g^2 - \|\mathbf{x} - \mathbf{c}_k\|_2^2))}$, using the property that $\sum_{i=1}^{C_g} \beta_i(\mathbf{x}) = 1$, by decomposing the approximation error into near and far components at a Euclidean radius of $2r_g$, we have

$$\begin{aligned} |\widehat{g}(\mathbf{x}) - g(\mathbf{x})| &= \left| \sum_{i=1}^{C_g} \beta_i(\mathbf{x}) (g(\mathbf{c}_i) - g(\mathbf{x})) \right| \\ &\leq \underbrace{\sum_{i: \|\mathbf{x} - \mathbf{c}_i\|_2 \leq 2r_g} \beta_i(\mathbf{x}) |g(\mathbf{x}) - g(\mathbf{c}_i)|}_{(I)} + \underbrace{\sum_{i: \|\mathbf{x} - \mathbf{c}_i\|_2 > 2r_g} \beta_i(\mathbf{x}) |g(\mathbf{x}) - g(\mathbf{c}_i)|}_{(II)}. \end{aligned}$$

For the near-center terms (I), we can bound the error using the intrinsic Hölder continuity. For sufficiently small ε such that $2r_g \leq \tau/2$, by Lemma 2, we have $d_{\mathcal{M}}(\mathbf{x}, \mathbf{c}_i) \leq 2\|\mathbf{x} - \mathbf{c}_i\|_2 \leq 4r_g$. Consequently, the intrinsic α -Hölder continuity yields

$$|g(\mathbf{x}) - g(\mathbf{c}_i)| \leq C_H (d_{\mathcal{M}}(\mathbf{x}, \mathbf{c}_i))^\alpha \leq C_H (4r_g)^\alpha \leq 4C_H r_g^\alpha,$$

since $4^\alpha \leq 4$ for $\alpha \in (0, 1]$. Thus

$$(I) \leq 4C_H r_g^\alpha \sum_i \beta_i(\mathbf{x}) \leq 4C_H r_g^\alpha.$$

For the far-center tail terms (II), the condition $\|\mathbf{x} - \mathbf{c}_i\|_2 > 2r_g$ implies $r_g^2 - \|\mathbf{x} - \mathbf{c}_i\|_2^2 < -3r_g^2$. Since $\|\mathbf{x} - \mathbf{c}_{i^*}\|_2 \leq r_g$, the denominator of the ambient Softmax POU $\beta_i(\mathbf{x})$ is bounded below

$$\sum_{k=1}^{C_g} \exp(M_g(r_g^2 - \|\mathbf{x} - \mathbf{c}_k\|_2^2)) \geq \exp(M_g(r_g^2 - \|\mathbf{x} - \mathbf{c}_{i^*}\|_2^2)) \geq \exp(0) = 1.$$

Applying the global bound $|g(\mathbf{x}) - g(\mathbf{c}_i)| \leq 2\|g\|_\infty$, the term (II) is bounded by

$$\begin{aligned}
(II) &= \sum_{i:\|\mathbf{x}-\mathbf{c}_i\|_2>2r_g} \frac{\exp(M_g(r_g^2 - \|\mathbf{x}-\mathbf{c}_i\|_2^2))}{\sum_{k=1}^{C_g} \exp(M_g(r_g^2 - \|\mathbf{x}-\mathbf{c}_k\|_2^2))} |g(\mathbf{x}) - g(\mathbf{c}_i)| \\
&\leq \sum_{i:\|\mathbf{x}-\mathbf{c}_i\|_2>2r_g} \exp(-3M_g r_g^2) \cdot 2\|g\|_\infty \\
&\leq 2C_g \|g\|_\infty \exp(-3M_g r_g^2).
\end{aligned}$$

Combining (I) and (II) yields

$$\sup_{\mathbf{x} \in \mathcal{M}} |\widehat{g}(\mathbf{x}) - g(\mathbf{x})| \leq 4C_H r_g^\alpha + 2C_g \|g\|_\infty \exp(-3M_g r_g^2). \quad (7)$$

Setting $r_g = (\varepsilon/(8C_H))^{1/\alpha}$ yields (I) $\leq \varepsilon/2$. By Lemma 2, the number of Euclidean balls of radius r_g required to cover \mathcal{M} is bounded by $C_g \leq C_{\mathcal{M}} r_g^{-d}$, where $C_{\mathcal{M}} = 3^d \text{Vol}(\mathcal{M}) d^{d/2}$. Substituting our choice of r_g , we obtain

$$C_g \leq C_{\mathcal{M}} \left(\left(\frac{\varepsilon}{8C_H} \right)^{1/\alpha} \right)^{-d} = C_{\mathcal{M}} (8C_H)^{d/\alpha} \varepsilon^{-\frac{d}{\alpha}}.$$

Finally, to guarantee (II) $\leq \varepsilon/2$, the scaling parameter must satisfy $M_g \geq (3r_g^2)^{-1} \log(4\|g\|_\infty C_g/\varepsilon)$. Substituting the explicit formulas for r_g and the upper bound for C_g , we require

$$\begin{aligned}
M_g &\geq \frac{(8C_H)^{2/\alpha}}{3} \varepsilon^{-\frac{2}{\alpha}} \log \left(4\|g\|_\infty C_{\mathcal{M}} (8C_H)^{d/\alpha} \varepsilon^{-\frac{d+\alpha}{\alpha}} \right) \\
&= \frac{(8C_H)^{2/\alpha}}{3} \varepsilon^{-\frac{2}{\alpha}} \left(\log \left(4\|g\|_\infty C_{\mathcal{M}} (8C_H)^{d/\alpha} \right) + \frac{d+\alpha}{\alpha} \log \frac{1}{\varepsilon} \right).
\end{aligned}$$

Assuming $\varepsilon \leq 1/e$ so that $\log(1/\varepsilon) \geq 1$, we can upper bound the bracketed sum by factoring out $\log(1/\varepsilon)$. Defining M_g as

$$M_g = \frac{(8C_H)^{2/\alpha}}{3} \left(\log \left(4\|g\|_\infty C_{\mathcal{M}} (8C_H)^{d/\alpha} \right) + \frac{d+\alpha}{\alpha} \right) \varepsilon^{-\frac{2}{\alpha}} \log \frac{1}{\varepsilon}$$

satisfies this condition, ensuring (II) $\leq \varepsilon/2$. This achieves the target uniform error $\sup_{\mathbf{x} \in \mathcal{M}} |\widehat{g}(\mathbf{x}) - g(\mathbf{x})| \leq \varepsilon$ and completes the proof. \square

A.3 Constructing Transformers for Softmax POU approximation: fundamental lemmas

This subsection details the structural lemmas (Lemmas 4, 5, 6, and 7) and their proofs. These proofs demonstrate how the native softmax attention mechanism in Transformers can realize our Softmax POU approximation framework. The pre-processing step embeds \mathbf{x} and an indicator exclusively into the first token, zero-pads the remaining sequence, and appends sinusoidal positional encodings across all P tokens.

Lemma 4 (Pre-processing Step). *Let $\mathbf{x} \in [0, 1]^d$ be the input vector, $P \geq 1$ be the sequence length, and $D = d + 4$ be the embedding dimension. There exists a pre-processing operator $\mathcal{P} : \mathbb{R}^d \rightarrow \mathbb{R}^{D \times P}$*

with the absolute values of the parameters bounded by 1, such that its output $\mathbf{Z}_0 = \mathcal{P}(\mathbf{x})$ is

$$\mathbf{Z}_0 = \begin{bmatrix} \mathbf{x} & \mathbf{0} & \cdots & \mathbf{0} \\ 1 & 0 & \cdots & 0 \\ 0 & 0 & \cdots & 0 \\ \sin(\theta_1) & \sin(\theta_2) & \cdots & \sin(\theta_P) \\ \cos(\theta_1) & \cos(\theta_2) & \cdots & \cos(\theta_P) \end{bmatrix} \in \mathbb{R}^{D \times P},$$

where $\theta_j = \frac{2\pi j}{P}$ for $j \in [P]$.

Proof of Lemma 4. Let $\mathbf{e}_1 = [1, 0, \dots, 0]^\top \in \mathbb{R}^P$ be the indicator vector for the first token. We construct the pre-processing operator as

$$\mathcal{P}(\mathbf{x}) = (\mathbf{W}_E \mathbf{x} + \mathbf{b}_E) \mathbf{e}_1^\top + \mathbf{P}.$$

We define the embedding weight matrix $\mathbf{W}_E \in \mathbb{R}^{D \times d}$ and the bias vector $\mathbf{b}_E \in \mathbb{R}^D$ as

$$\mathbf{W}_E = \begin{bmatrix} \mathbf{I}_d \\ \mathbf{0}_{1 \times d} \\ \mathbf{0}_{1 \times d} \\ \mathbf{0}_{2 \times d} \end{bmatrix}, \quad \mathbf{b}_E = \begin{bmatrix} \mathbf{0}_{d \times 1} \\ 1 \\ 0 \\ \mathbf{0}_{2 \times 1} \end{bmatrix},$$

and the positional encoding matrix $\mathbf{P} \in \mathbb{R}^{D \times P}$ as

$$\mathbf{P} = \begin{bmatrix} \mathbf{0}_{d \times P} \\ \mathbf{0}_{1 \times P} \\ \mathbf{0}_{1 \times P} \\ \sin(\theta_1) & \cdots & \sin(\theta_P) \\ \cos(\theta_1) & \cdots & \cos(\theta_P) \end{bmatrix},$$

where $\theta_j = \frac{2\pi j}{P}$ for $j \in [P]$. Therefore, we have

$$\mathbf{Z}_0 = \mathcal{P}(\mathbf{x}) = \begin{bmatrix} \mathbf{x} & \mathbf{0} & \cdots & \mathbf{0} \\ 1 & 0 & \cdots & 0 \\ 0 & 0 & \cdots & 0 \\ \sin(\theta_1) & \sin(\theta_2) & \cdots & \sin(\theta_P) \\ \cos(\theta_1) & \cos(\theta_2) & \cdots & \cos(\theta_P) \end{bmatrix} \in \mathbb{R}^{D \times P},$$

thus we complete the proof. \square

The first MHA layer extracts two affine transformation features, while the exact angular identity θ_j of the sinusoidal positional encodings remains invariant up to a uniform scalar scaling.

Lemma 5 (Parallel Affine Transformations via MHA). *Let $\mathbf{Z}_0 \in \mathbb{R}^{D \times P}$ ($D = d + 4$) as defined in Lemma 4. For target affine functions $T_h(\mathbf{x}) = \boldsymbol{\xi}_h^\top \mathbf{x} + b_h$ and $R_h(\mathbf{x}) = \boldsymbol{\zeta}_h^\top \mathbf{x} + c_h$ ($h \in [P]$), let $B_T := \max_h \|T_h\|_\infty$, $B_R := \max_h \|R_h\|_\infty$, and $B_{\mathcal{A}_1} := \max_h \max\{\|\boldsymbol{\xi}_h\|_\infty, \|\boldsymbol{\zeta}_h\|_\infty, |b_h|, |c_h|\}$. There exists an MHA layer $\mathcal{A}_1 : \mathbb{R}^{D \times P} \rightarrow \mathbb{R}^{D \times P}$ with $H = P + 2$ heads, $d_v = d_k = 2$, and scaling factor*

$M > 0$, yielding output $\widehat{\mathbf{Z}}_1 = \mathcal{A}_1(\mathbf{Z}_0) \in \mathbb{R}^{D \times P}$ whose j -th column is

$$(\widehat{\mathbf{Z}}_1)_{:,j} = \begin{bmatrix} \widetilde{T}_j(\mathbf{x}) \\ \widetilde{R}_j(\mathbf{x}) \\ \mathbf{0}_{d-1} \\ \widetilde{I}_j \\ \lambda(M) \sin(\theta_j) \\ \lambda(M) \cos(\theta_j) \end{bmatrix}, \quad \forall j \in [P].$$

Let $c = 1 - \cos(2\pi/P) > 0$. The output components and parameter magnitude satisfy

1. **Affine Outputs:** we have the approximation error

$$\begin{aligned} |T_j(\mathbf{x}) - \widetilde{T}_j(\mathbf{x})| &\leq (P-1)B_T e^{-cM}, \\ |R_j(\mathbf{x}) - \widetilde{R}_j(\mathbf{x})| &\leq (P-1)B_R e^{-cM}. \end{aligned}$$

2. **Indicator Output:** $\widetilde{I}_1 = \eta(M) := \frac{e^M}{\sum_{l=1}^P e^{M \cos(\theta_l)}}$, and

$$\begin{aligned} 0 \leq 1 - \widetilde{I}_1 = 1 - \eta(M) &\leq (P-1)e^{-cM}, & (j=1) \\ 0 \leq \widetilde{I}_j &\leq e^{-cM}. & (j \neq 1) \end{aligned}$$

3. **PE Output:** the scaling coefficient $\lambda(M)$ satisfies

$$\lambda(M) := \frac{\sum_{k=1}^P e^{M \cos(\theta_k)} \cos(\theta_k)}{\sum_{l=1}^P e^{M \cos(\theta_l)}}, \quad 0 \leq 1 - \lambda(M) \leq 2(P-1)e^{-cM}.$$

4. **Parameter Bounds:** the maximum parameter magnitude M_{A_1} satisfy

$$M_{A_1} \leq \max \{1, M, (1 + (P-1)e^{-cM})B_{A_1}\}.$$

Proof of Lemma 5. We set the uniform dimension for query, key, and value matrices to $d_k = 2$ and $d_v = 2$.

Step 1: Affine Heads ($h \in [P]$). We construct the first P heads in the first encoder block to selectively route the affine transformations. We define the 2D rotation matrix $\mathbf{R}(\theta)$ as

$$\mathbf{R}(\theta) = \begin{bmatrix} \cos \theta & \sin \theta \\ -\sin \theta & \cos \theta \end{bmatrix}.$$

Before defining the attention matrices, we introduce a deterministic scalar $\eta(M)$ representing the exact peak attention weight, that is

$$\eta(M) := \frac{e^M}{\sum_{l=1}^P e^{M \cos(\theta_l)}}.$$

To eliminate the influence of the attention matrix while realizing affine transformations, we preemptively rescale the value matrix by $\eta(M)^{-1}$. Adhering to the uniform value dimension $d_v = 2$,

we stack the weights and biases of both affine transformations. The query, key, and value matrices ($\mathbf{Q}_1^h, \mathbf{K}_1^h, \mathbf{V}_1^h \in \mathbb{R}^{2 \times D}$) are defined as

$$\begin{aligned}\mathbf{Q}_1^h &= [\mathbf{0}_{2 \times d} \quad \mathbf{0}_{2 \times 2} \quad \mathbf{R}(\theta_1 - \theta_h)] \implies (\mathbf{Q}_1^h \mathbf{Z}_0)_{:,j} = \begin{bmatrix} \sin(\theta_j + \theta_1 - \theta_h) \\ \cos(\theta_j + \theta_1 - \theta_h) \end{bmatrix}, \\ \mathbf{K}_1^h &= [\mathbf{0}_{2 \times d} \quad \mathbf{0}_{2 \times 2} \quad M \mathbf{I}_2] \implies (\mathbf{K}_1^h \mathbf{Z}_0)_{:,k} = \begin{bmatrix} M \sin(\theta_k) \\ M \cos(\theta_k) \end{bmatrix}, \\ \mathbf{V}_1^h &= \frac{1}{\eta(M)} \begin{bmatrix} \boldsymbol{\xi}_h^\top & b_h & \mathbf{0}_{1 \times 3} \\ \boldsymbol{\zeta}_h^\top & c_h & \mathbf{0}_{1 \times 3} \end{bmatrix} \\ &\implies (\mathbf{V}_1^h \mathbf{Z}_0)_{:,k} = \frac{1}{\eta(M)} \begin{bmatrix} \boldsymbol{\xi}_h^\top \mathbf{x} + b_h \\ \boldsymbol{\zeta}_h^\top \mathbf{x} + c_h \end{bmatrix} \delta_{k,1} = \frac{1}{\eta(M)} \begin{bmatrix} T_h(\mathbf{x}) \\ R_h(\mathbf{x}) \end{bmatrix} \delta_{k,1}.\end{aligned}$$

Following the attention mechanism, the unnormalized score $s_{k,j}^h$ is defined as the inner product between the k -th key column and the j -th query column, that is,

$$s_{k,j}^h = (\mathbf{K}_1^h \mathbf{Z}_0)_{:,k}^\top (\mathbf{Q}_1^h \mathbf{Z}_0)_{:,j} = M \cos(\theta_k - (\theta_j + \theta_1 - \theta_h)).$$

Consequently, the (k, j) -th entry of the attention matrix $\mathbf{A}_1^h \in \mathbb{R}^{P \times P}$ is computed via the column-wise softmax function, we have

$$(\mathbf{A}_1^h)_{k,j} = \frac{\exp(s_{k,j}^h)}{S_j}, \quad \text{where } S_j = \sum_{l=1}^P \exp(s_{l,j}^h).$$

Let $c = 1 - \cos(2\pi/P) > 0$ denote the spectral gap. For any $\theta_a \neq \theta_b$, we have $\cos(\theta_a - \theta_b) \leq 1 - c$. We analyze the columns of \mathbf{A}_1^h (indexed by the query token j) by bounding the numerator and the denominator S_j in the following.

- **Target Column ($j = h$):** The relative phase shift perfectly aligns the attention peak with the source key $k = 1$. Substituting $j = h$ yields $s_{k,h}^h = M \cos(\theta_k - \theta_1)$. For the source key ($k = 1$), the score reaches its exact maximum $s_{1,h}^h = M \cos(0) = M$. For the denominator $S_h = \sum_{l=1}^P e^{M \cos(\theta_l - \theta_1)}$, subtracting the constant phase θ_1 merely applies a cyclic permutation to the uniform grid. Due to the shift-invariance of the periodic grid, we have $S_h = \sum_{l=1}^P e^{M \cos(\theta_l)}$. Thus, the attention weight for the source key is

$$(\mathbf{A}_1^h)_{1,h} = \frac{e^{s_{1,h}^h}}{S_h} = \frac{e^M}{\sum_{l=1}^P e^{M \cos(\theta_l)}} = \eta(M),$$

therefore, we have

$$(\mathbf{V}_1^h \mathbf{Z}_0)_{:,1} (\mathbf{A}_1^h)_{1,h} = \eta(M) \cdot \frac{1}{\eta(M)} \begin{bmatrix} T_h(\mathbf{x}) \\ R_h(\mathbf{x}) \end{bmatrix} = \begin{bmatrix} T_h(\mathbf{x}) \\ R_h(\mathbf{x}) \end{bmatrix}.$$

Because $(\mathbf{V}_1^h \mathbf{Z}_0)_{:,k} = \mathbf{0}$ for $k \neq 1$, we get

$$(\mathbf{V}_1^h \mathbf{Z}_0) (\mathbf{A}_1^h)_{:,h} = \sum_{k=1}^P (\mathbf{A}_1^h)_{k,h} (\mathbf{V}_1^h \mathbf{Z}_0)_{:,k} = (\mathbf{A}_1^h)_{1,h} (\mathbf{V}_1^h \mathbf{Z}_0)_{:,1} = \begin{bmatrix} T_h(\mathbf{x}) \\ R_h(\mathbf{x}) \end{bmatrix}.$$

- **Other Columns** ($j \neq h$): The query perfectly matches a shifted key position k^* satisfying $\theta_{k^*} \equiv \theta_j + \theta_1 - \theta_h$. Since the target differs ($j \neq h$), the attention peak shifts away from the source token ($k^* \neq 1$). The unnormalized attention score at the source key ($k = 1$) is

$$s_{1,j}^h = M \cos(\theta_1 - (\theta_j + \theta_1 - \theta_h)) = M \cos(\theta_h - \theta_j) \leq M(1 - c).$$

We denote the output for these non-target columns as $(\mathbf{V}_1^h \mathbf{Z}_0)(\mathbf{A}_1^h)_{:,j} := [\epsilon_{h,j}, \tilde{\epsilon}_{h,j}]^\top$, then

$$\begin{aligned} \begin{bmatrix} \epsilon_{h,j} \\ \tilde{\epsilon}_{h,j} \end{bmatrix} &= (\mathbf{V}_1^h \mathbf{Z}_0)(\mathbf{A}_1^h)_{:,j} = \sum_{k=1}^P (\mathbf{V}_1^h \mathbf{Z}_0)_{:,k} (\mathbf{A}_1^h)_{k,j} \\ &= (\mathbf{V}_1^h \mathbf{Z}_0)_{:,1} (\mathbf{A}_1^h)_{1,j} = \frac{(\mathbf{A}_1^h)_{1,j}}{\eta(M)} \begin{bmatrix} T_h(\mathbf{x}) \\ R_h(\mathbf{x}) \end{bmatrix}. \end{aligned}$$

Due to the exact shift-invariance, $S_j = \sum_{l=1}^P e^{M \cos(\theta_l - \theta_j)} = \sum_{l=1}^P e^{M \cos(\theta_l)} \equiv S_h$, thus

$$\begin{aligned} \epsilon_{h,j} &= \frac{e^{s_{1,j}^h} / S_j}{e^M / S_h} T_h(\mathbf{x}) = e^{s_{1,j}^h - M} T_h(\mathbf{x}) \implies |\epsilon_{h,j}| \leq e^{M(1-c) - M} B_T = e^{-cM} B_T, \\ \tilde{\epsilon}_{h,j} &= \frac{e^{s_{1,j}^h} / S_j}{e^M / S_h} R_h(\mathbf{x}) = e^{s_{1,j}^h - M} R_h(\mathbf{x}) \implies |\tilde{\epsilon}_{h,j}| \leq e^{M(1-c) - M} B_R = e^{-cM} B_R. \end{aligned}$$

Step 2: Indicator & Positional Encoding Heads ($h \in \{P+1, P+2\}$). We dedicate Head $P+1$ to preserve the indicator $\delta_{j,1}$ and Head $P+2$ to preserve the positional encodings. The query, key, and value matrices ($\mathbf{Q}_1^h, \mathbf{K}_1^h, \mathbf{V}_1^h \in \mathbb{R}^{2 \times D}$) are defined as

$$\begin{aligned} \mathbf{Q}_1^h &= [\mathbf{0}_{2 \times d} \quad \mathbf{0}_{2 \times 2} \quad \mathbf{I}_2] \implies (\mathbf{Q}_1^h \mathbf{Z}_0)_{:,j} = \begin{bmatrix} \sin(\theta_j) \\ \cos(\theta_j) \end{bmatrix}, \quad \forall h \in \{P+1, P+2\}, \\ \mathbf{K}_1^h &= [\mathbf{0}_{2 \times d} \quad \mathbf{0}_{2 \times 2} \quad M \mathbf{I}_2] \implies (\mathbf{K}_1^h \mathbf{Z}_0)_{:,k} = \begin{bmatrix} M \sin(\theta_k) \\ M \cos(\theta_k) \end{bmatrix}, \quad \forall h \in \{P+1, P+2\}, \\ \mathbf{V}_1^{P+1} &= \begin{bmatrix} \mathbf{0}_{1 \times d} & 1 & \mathbf{0}_{1 \times 3} \\ \mathbf{0}_{1 \times d} & 0 & \mathbf{0}_{1 \times 3} \end{bmatrix} \implies (\mathbf{V}_1^{P+1} \mathbf{Z}_0)_{:,k} = \begin{bmatrix} \delta_{k,1} \\ 0 \end{bmatrix}, \\ \mathbf{V}_1^{P+2} &= [\mathbf{0}_{2 \times d} \quad \mathbf{0}_{2 \times 2} \quad \mathbf{I}_2] \implies (\mathbf{V}_1^{P+2} \mathbf{Z}_0)_{:,k} = \begin{bmatrix} \sin(\theta_k) \\ \cos(\theta_k) \end{bmatrix}. \end{aligned}$$

The shared unnormalized attention score is given by

$$s_{k,j}^{\text{id}} = (\mathbf{K}_1^h \mathbf{Z}_0)_{:,k}^\top (\mathbf{Q}_1^h \mathbf{Z}_0)_{:,j} = M(\sin(\theta_j) \sin(\theta_k) + \cos(\theta_j) \cos(\theta_k)) = M \cos(\theta_j - \theta_k).$$

The corresponding attention weight is $(\mathbf{A}^{\text{id}})_{k,j} = \frac{\exp(M \cos(\theta_j - \theta_k))}{S^{\text{id}}}$. Due to the symmetry of the uniform periodic grid, the normalization denominator S^{id} is invariant to the query index j . By applying a periodic shift to the summation index, it simplifies to

$$S^{\text{id}} = \sum_{l=1}^P \exp(M \cos(\theta_j - \theta_l)) = \sum_{l=1}^P \exp(M \cos(\theta_l)).$$

For the indicator head ($h = P+1$), to align with $d_v = 2$, we pad the indicator value with a

zero row, making the value vector $[\delta_{k,1}, 0]^\top$. Thus, the output for the j -th token is $[\tilde{I}_j, 0]^\top$, where the first component \tilde{I}_j evaluates to

$$\tilde{I}_j = \sum_{k=1}^P (\mathbf{A}^{\text{id}})_{k,j} \delta_{k,1} = (\mathbf{A}^{\text{id}})_{1,j} = \frac{e^{M \cos(\theta_j - \theta_1)}}{\sum_{l=1}^P e^{M \cos(\theta_l)}}.$$

For the source token ($j = 1$), the numerator is e^M . We define this exact output as a deterministic scalar coefficient $\eta(M)$ that

$$\tilde{I}_1 = \eta(M) := \frac{e^M}{\sum_{l=1}^P e^{M \cos(\theta_l)}}.$$

By bounding the $P - 1$ off-diagonal terms in the denominator by $e^{M(1-c)}$, we get

$$\eta(M) \geq \frac{e^M}{e^M + (P-1)e^{M(1-c)}} \implies 0 \leq 1 - \eta(M) \leq (P-1)e^{-cM}.$$

For non-source tokens ($j \neq 1$), the numerator is bounded by $e^{M(1-c)}$ while the denominator is at least e^M , we have

$$\tilde{I}_j \leq \frac{e^{M(1-c)}}{e^M} = e^{-cM}.$$

This deterministic scalar $\eta(M)$ allows the subsequent point-wise FFN layer to restore the indicator to 1.

For the PE head ($h = P + 2$), the value vector is $[\sin(\theta_k), \cos(\theta_k)]^\top$. By substituting the relative phase $\phi_k = \theta_k - \theta_j$, the output for the j -th token becomes

$$\begin{aligned} \sum_{k=1}^P (\mathbf{A}^{\text{id}})_{k,j} \begin{bmatrix} \sin(\theta_k) \\ \cos(\theta_k) \end{bmatrix} &= \frac{1}{S^{\text{id}}} \sum_{k=1}^P e^{M \cos(\phi_k)} \begin{bmatrix} \sin(\phi_k + \theta_j) \\ \cos(\phi_k + \theta_j) \end{bmatrix} \\ &= \frac{1}{S^{\text{id}}} \sum_{k=1}^P e^{M \cos(\phi_k)} \begin{bmatrix} \sin(\phi_k) \cos(\theta_j) + \cos(\phi_k) \sin(\theta_j) \\ \cos(\phi_k) \cos(\theta_j) - \sin(\phi_k) \sin(\theta_j) \end{bmatrix}. \end{aligned}$$

Since subtracting the grid point θ_j applies a cyclic permutation, the relative phases reconstruct the identical equispaced grid of base angles. Specifically, evaluated as an unordered set modulo 2π , we have the set equality: $\Phi = \{\phi_k \pmod{2\pi}\}_{k=1}^P = \left\{ \frac{2\pi(k-1)}{P} \right\}_{k=1}^P = \{\theta_k\}_{k=1}^P$. Defining the summand $g(\phi) = e^{M \cos(\phi)} \sin(\phi)$, we partition the grid Φ into self-conjugate poles $\Phi_0 = \Phi \cap \{\pi, 2\pi\}$ (where $\pi \in \Phi$ if and only if P is even) and the remaining conjugate pairs $\{\phi, 2\pi - \phi\}$. For $\phi \in \Phi_0$, the term disappears trivially since $g(0) = g(\pi) = 0$. For any conjugate pair, we have

$$g(2\pi - \phi) + g(\phi) = e^{M \cos(\phi)} (-\sin(\phi) + \sin(\phi)) = 0.$$

Thus, regardless of the parity of P , the global summation becomes

$$\sum_{k=1}^P e^{M \cos(\phi_k)} \sin(\phi_k) = \sum_{\phi \in \Phi_0} g(\phi) + \frac{1}{2} \sum_{\phi \notin \Phi_0} (g(\phi) + g(2\pi - \phi)) = 0.$$

Hence, utilizing the established set equality $\Phi = \{\theta_l\}_{l=1}^P$, the output for j -th token simplifies to a

scaled version of the input positional encoding, that is

$$\left(\frac{\sum_{l=1}^P e^{M \cos(\theta_l)} \cos(\theta_l)}{\sum_{l=1}^P e^{M \cos(\theta_l)}} \right) \begin{bmatrix} \sin(\theta_j) \\ \cos(\theta_j) \end{bmatrix} = \lambda(M) \begin{bmatrix} \sin(\theta_j) \\ \cos(\theta_j) \end{bmatrix}.$$

Considering $1 - \lambda(M) = \frac{\sum_{l=1}^P e^{M \cos(\theta_l)} (1 - \cos(\theta_l))}{\sum_{l=1}^P e^{M \cos(\theta_l)}}$, for the peak term where $\theta_l = 0$ (corresponding to $l = P$), the numerator term is $e^M (1 - \cos(0)) = 0$. For the remaining $P - 1$ terms ($l \neq P$), we have $e^{M \cos(\theta_l)} \leq e^{M(1-c)}$ and $(1 - \cos(\theta_l)) \leq 2$. Lower bounding the denominator by the single peak term e^M , we obtain

$$0 \leq 1 - \lambda(M) \leq \frac{(P-1) \cdot e^{M(1-c)} \cdot 2}{e^M} = 2(P-1)e^{-cM}.$$

Thus, positional encodings are preserved with a uniform scaling coefficient $\lambda(M)$, allowing easy restoration in the following point-wise FFN layer.

Step 3: Output Projection and Error Bounds. Concatenating the outputs of all $P + 2$ heads yields the intermediate matrix $\mathbf{C} \in \mathbb{R}^{2(P+2) \times P}$ in the following form

$$\mathbf{C} = \begin{bmatrix} T_1(\mathbf{x}) & \epsilon_{1,2} & \dots & \epsilon_{1,P} \\ R_1(\mathbf{x}) & \tilde{\epsilon}_{1,2} & \dots & \tilde{\epsilon}_{1,P} \\ \epsilon_{2,1} & T_2(\mathbf{x}) & \dots & \epsilon_{2,P} \\ \tilde{\epsilon}_{2,1} & R_2(\mathbf{x}) & \dots & \tilde{\epsilon}_{2,P} \\ \vdots & \vdots & \ddots & \vdots \\ \epsilon_{P,1} & \epsilon_{P,2} & \dots & T_P(\mathbf{x}) \\ \tilde{\epsilon}_{P,1} & \tilde{\epsilon}_{P,2} & \dots & R_P(\mathbf{x}) \\ \tilde{I}_1 & \tilde{I}_2 & \dots & \tilde{I}_P \\ 0 & 0 & \dots & 0 \\ \lambda(M) \sin(\theta_1) & \lambda(M) \sin(\theta_2) & \dots & \lambda(M) \sin(\theta_P) \\ \lambda(M) \cos(\theta_1) & \lambda(M) \cos(\theta_2) & \dots & \lambda(M) \cos(\theta_P) \end{bmatrix}.$$

By introducing the block identity matrix $[\mathbf{I}_2 \ \dots \ \mathbf{I}_2] \in \mathbb{R}^{2 \times 2P}$, we choose the output projection matrix $\mathbf{W}^O \in \mathbb{R}^{D \times 2(P+2)}$ as

$$\mathbf{W}^O = \begin{bmatrix} [\mathbf{I}_2 \ \dots \ \mathbf{I}_2] & \mathbf{0}_{2 \times 2} & \mathbf{0}_{2 \times 2} \\ \mathbf{0}_{(d-1) \times 2P} & \mathbf{0}_{(d-1) \times 2} & \mathbf{0}_{(d-1) \times 2} \\ \mathbf{0}_{1 \times 2P} & \begin{bmatrix} 1 & 0 \end{bmatrix} & \mathbf{0}_{1 \times 2} \\ \mathbf{0}_{2 \times 2P} & \mathbf{0}_{2 \times 2} & \mathbf{I}_2 \end{bmatrix},$$

the MHA output for the j -th token is

$$(\hat{\mathbf{Z}}_1)_{:,j} = \mathbf{W}^O \mathbf{C}_{:,j} = \begin{bmatrix} \tilde{T}_j(\mathbf{x}) \\ \tilde{R}_j(\mathbf{x}) \\ \mathbf{0}_{d-1} \\ \tilde{I}_j \\ \lambda(M) \begin{bmatrix} \sin(\theta_j) \\ \cos(\theta_j) \end{bmatrix} \end{bmatrix},$$

where

$$\tilde{T}_j(\mathbf{x}) = T_j(\mathbf{x}) + \sum_{h \neq j} \epsilon_{h,j}, \quad \tilde{R}_j(\mathbf{x}) = R_j(\mathbf{x}) + \sum_{h \neq j} \tilde{\epsilon}_{h,j}.$$

Given the uniform bounds $|\epsilon_{h,j}| \leq e^{-cM} B_T$ and $|\tilde{\epsilon}_{h,j}| \leq e^{-cM} B_R$, we have

$$\begin{aligned} |\tilde{T}_j(\mathbf{x}) - T_j(\mathbf{x})| &= \left| \sum_{h \neq j} \epsilon_{h,j} \right| \leq \sum_{h \neq j} |\epsilon_{h,j}| \leq (P-1)e^{-cM} B_T, \\ |\tilde{R}_j(\mathbf{x}) - R_j(\mathbf{x})| &= \left| \sum_{h \neq j} \tilde{\epsilon}_{h,j} \right| \leq \sum_{h \neq j} |\tilde{\epsilon}_{h,j}| \leq (P-1)e^{-cM} B_R. \end{aligned}$$

Step 4: Parameter Bounds. To bound the parameter magnitude, we evaluate the maximum absolute entry $\|\cdot\|_{\max}$ for each parameter matrix over all heads $h \in [P+2]$. The peak attention weight satisfies $\eta(M)^{-1} \leq \frac{e^{M+(P-1)e^{M(1-c)}}}{e^M} = 1 + (P-1)e^{-cM}$. It follows that the maximum entries are explicitly bounded by

$$\begin{aligned} \max_h \|\mathbf{Q}_1^h\|_{\max} &\leq 1, \\ \max_h \|\mathbf{K}_1^h\|_{\max} &= M, \\ \max_h \|\mathbf{V}_1^h\|_{\max} &\leq \max\{1, \eta(M)^{-1} B_{\mathcal{A}_1}\} \leq \max\{1, (1 + (P-1)e^{-cM}) B_{\mathcal{A}_1}\}, \\ \|\mathbf{W}^O\|_{\max} &= 1. \end{aligned}$$

Therefore, the maximum absolute value of any parameter in the MHA layer \mathcal{A}_1 , denoted as $M_{\mathcal{A}_1}$, is bounded by

$$\begin{aligned} M_{\mathcal{A}_1} &= \max\left\{ \max_h \|\mathbf{Q}_1^h\|_{\max}, \max_h \|\mathbf{K}_1^h\|_{\max}, \max_h \|\mathbf{V}_1^h\|_{\max}, \|\mathbf{W}^O\|_{\max} \right\} \\ &\leq \max\{1, M, (1 + (P-1)e^{-cM}) B_{\mathcal{A}_1}\}. \end{aligned}$$

Thus, we complete the proof. \square

The first point-wise FFN layer acts as a precise non-linear denoiser, leveraging the hard-thresholding property of ReLU activations to completely eliminate small errors and recover the canonical form and original sinusoidal positional encodings.

Lemma 6 (FFN Exact Thresholding and Restoration). *Let $\hat{\mathbf{Z}}_1 \in \mathbb{R}^{D \times P}$ (where $D = d + 4$) be the output matrix from the MHA layer defined in Lemma 5. Assume M is sufficiently large such that $(P+1)e^{-cM} < 1$. There exists a point-wise FFN layer $\mathcal{F}_1 : \mathbb{R}^{D \times P} \rightarrow \mathbb{R}^{D \times P}$ with hidden dimension $d_{\text{ff}} = 2D = 2d + 8$, such that its output $\mathbf{Z}_1 = \mathcal{F}_1(\hat{\mathbf{Z}}_1) \in \mathbb{R}^{D \times P}$ takes the column-wise form*

$$(\mathbf{Z}_1)_{:,j} = \begin{bmatrix} \tilde{T}_j(\mathbf{x}) \\ \tilde{R}_j(\mathbf{x}) \\ \mathbf{0}_{d-1} \\ \delta_{j,1} \\ \sin(\theta_j) \\ \cos(\theta_j) \end{bmatrix}, \quad \forall j \in [P].$$

The maximum parameter magnitude $M_{\mathcal{F}_1}$ satisfy

$$M_{\mathcal{F}_1} \leq \frac{1}{1 - 2Pe^{-cM}}.$$

Proof of Lemma 6. Let $w_{\text{ind}} = \frac{1}{\eta(M) - 2e^{-cM}}$. We define the j -th column of the input as $\widehat{\mathbf{z}}_j = (\widehat{\mathbf{Z}}_1)_{:,j}$ and the j -th column of the output as $\mathbf{z}_j = (\mathbf{Z}_1)_{:,j}$. We construct the FFN applied to each column as $\mathbf{z}_j = \mathbf{W}_2 \sigma(\mathbf{W}_1 \widehat{\mathbf{z}}_j + \mathbf{b}_1)$.

To uniformly map the D -dimensional input across the $2D$ hidden neurons, we introduce a diagonal scaling matrix $\mathbf{\Lambda} \in \mathbb{R}^{D \times D}$ defined as

$$\mathbf{\Lambda} = \text{diag}\left(\underbrace{1, \dots, 1}_{d+1}, w_{\text{ind}}, \frac{1}{\lambda(M)}, \frac{1}{\lambda(M)}\right).$$

We set the weights $\mathbf{W}_1 \in \mathbb{R}^{2D \times D}$, $\mathbf{W}_2 \in \mathbb{R}^{D \times 2D}$ and biases $\mathbf{b}_1 \in \mathbb{R}^{2D}$, $\mathbf{b}_2 \in \mathbb{R}^D$ as

$$\begin{aligned} \mathbf{W}_1 &= \begin{bmatrix} \mathbf{I}_D \\ -\mathbf{I}_D \end{bmatrix}, & \mathbf{b}_1 &= \begin{bmatrix} -2e^{-cM} \mathbf{e}_{d+2} \\ \mathbf{0}_D \end{bmatrix}, \\ \mathbf{W}_2 &= [\mathbf{\Lambda} \quad -\mathbf{\Lambda}], & \mathbf{b}_2 &= \mathbf{0}_D, \end{aligned}$$

where $\mathbf{e}_{d+2} \in \mathbb{R}^D$ is the standard basis vector for the $(d+2)$ -th component.

Using the ReLU identity $x = \sigma(x) - \sigma(-x)$, we analyze the output column \mathbf{z}_j . By evaluating $\mathbf{z}_j = \mathbf{\Lambda} \sigma(\widehat{\mathbf{z}}_j - 2e^{-cM} \mathbf{e}_{d+2}) - \mathbf{\Lambda} \sigma(-\widehat{\mathbf{z}}_j)$ component-wise, we get

$$\begin{aligned} (\mathbf{z}_j)_{1:d+1} &= \sigma((\widehat{\mathbf{z}}_j)_{1:d+1}) - \sigma(-(\widehat{\mathbf{z}}_j)_{1:d+1}) = (\widehat{\mathbf{z}}_j)_{1:d+1}, \\ (\mathbf{z}_j)_{d+3:d+4} &= \frac{1}{\lambda(M)} (\sigma((\widehat{\mathbf{z}}_j)_{d+3:d+4}) - \sigma(-(\widehat{\mathbf{z}}_j)_{d+3:d+4})) = \frac{1}{\lambda(M)} (\widehat{\mathbf{z}}_j)_{d+3:d+4}. \end{aligned}$$

For the indicator neuron (index $d+2$), since $\widetilde{I}_j \geq 0$, the negative channel trivially evaluates to $\sigma(-\widetilde{I}_j) = 0$. Thus, substituting $(\widehat{\mathbf{z}}_j)_{d+2} = \widetilde{I}_j$ yields

$$\begin{aligned} (\mathbf{z}_j)_{d+2} &= w_{\text{ind}} \cdot \sigma(\widetilde{I}_j - 2e^{-cM}) - 0 \\ &= \begin{cases} w_{\text{ind}} \cdot \sigma(\eta(M) - 2e^{-cM}) = 1, & \text{if } j = 1, \\ w_{\text{ind}} \cdot \sigma(\widetilde{I}_j - 2e^{-cM}) = 0, & \text{if } j \neq 1 \text{ (since } \widetilde{I}_j \leq e^{-cM}), \end{cases} \end{aligned}$$

yielding $(\mathbf{z}_j)_{d+2} = \delta_{j,1}$. Concatenating all evaluated components, the exact restored output column is precisely $\mathbf{z}_j = [\widetilde{T}_j(\mathbf{x}), \widetilde{R}_j(\mathbf{x}), \mathbf{0}_{d-1}^\top, \delta_{j,1}, \sin(\theta_j), \cos(\theta_j)]^\top$.

Using the bounds $\lambda(M) \geq 1 - 2(P-1)e^{-cM}$ and $\eta(M) \geq 1 - (P-1)e^{-cM}$ from Lemma 5, the parameter magnitude is bounded by the maximum entry in $\mathbf{\Lambda}$ and \mathbf{b}_1 :

$$\begin{aligned} M_{\mathcal{F}_1} &= \max \left\{ 1, \frac{1}{\lambda(M)}, \frac{1}{\eta(M) - 2e^{-cM}}, 2e^{-cM} \right\} \\ &\leq \max \left\{ \frac{1}{1 - 2(P-1)e^{-cM}}, \frac{1}{1 - (P+1)e^{-cM}} \right\} \leq \frac{1}{1 - 2Pe^{-cM}}, \end{aligned}$$

where the constants 1 and $2e^{-cM}$ are absorbed since the upper bound is strictly greater than 1. \square

The second MHA layer aggregates local affine transformation features to a global approximant via softmax attention mechanism, utilizing $\tilde{T}_j(\mathbf{x})$ as local spatial features and $\tilde{R}_j(\mathbf{x})$ as local approximation expert features.

Lemma 7 (Softmax POU via MHA). *Let $\mathbf{Z}_1 \in \mathbb{R}^{D \times P}$ (where $D = d+4$) be the output matrix from the FFN layer defined in Lemma 6. There exists a single-head MHA layer $\mathcal{A}_2 : \mathbb{R}^{D \times P} \rightarrow \mathbb{R}^{D \times P}$ with $H = 1$ and $d_k = d_v = 1$, yielding output $\hat{\mathbf{Z}}_2 = \mathcal{A}_2(\mathbf{Z}_1) \in \mathbb{R}^{D \times P}$ such that its first column ($k = 1$) evaluates to*

$$(\hat{\mathbf{Z}}_2)_{:,1} = \begin{bmatrix} \hat{g}_T(\mathbf{x}) \\ \mathbf{0}_{D-1} \end{bmatrix} = \hat{g}_T(\mathbf{x})\mathbf{e}_1,$$

where

$$\hat{g}_T(\mathbf{x}) := \sum_{j=1}^P \tilde{\beta}_j(\mathbf{x})\tilde{R}_j(\mathbf{x}), \quad \tilde{\beta}_j(\mathbf{x}) := \frac{\exp(\tilde{T}_j(\mathbf{x}))}{\sum_{l=1}^P \exp(\tilde{T}_l(\mathbf{x}))},$$

and all other columns ($k \neq 1$) evaluate to constant vectors $\tilde{R}(\mathbf{x})\mathbf{e}_1$, where $\tilde{R}(\mathbf{x}) = \frac{1}{P} \sum_{j=1}^P \tilde{R}_j(\mathbf{x})$. The maximum parameter magnitude $M_{\mathcal{A}_2}$ satisfy

$$M_{\mathcal{A}_2} = 1.$$

Proof of Lemma 7. We use a single attention head ($H = 1$) with $d_k = d_v = 1$. Let $\mathbf{e}_1, \mathbf{e}_2, \mathbf{e}_{d+2} \in \mathbb{R}^D$ be the standard basis vectors. We define the projection matrices $\mathbf{Q}_2^1, \mathbf{K}_2^1, \mathbf{V}_2^1 \in \mathbb{R}^{1 \times D}$ as

$$\begin{aligned} \mathbf{Q}_2^1 = \mathbf{e}_{d+2}^\top &\implies (\mathbf{Q}_2^1 \mathbf{Z}_1)_{:,j} = \delta_{j,1}, \\ \mathbf{K}_2^1 = \mathbf{e}_1^\top &\implies (\mathbf{K}_2^1 \mathbf{Z}_1)_{:,k} = \tilde{T}_k(\mathbf{x}), \\ \mathbf{V}_2^1 = \mathbf{e}_2^\top &\implies (\mathbf{V}_2^1 \mathbf{Z}_1)_{:,k} = \tilde{R}_k(\mathbf{x}). \end{aligned}$$

The unnormalized attention score $s_{k,j} = (\mathbf{K}_2^1 \mathbf{Z}_1)_{:,k}^\top (\mathbf{Q}_2^1 \mathbf{Z}_1)_{:,j}$ evaluates to

$$s_{k,j} = \tilde{T}_k(\mathbf{x}) \cdot \delta_{j,1} = \begin{cases} \tilde{T}_k(\mathbf{x}), & j = 1, \\ 0, & j \neq 1. \end{cases}$$

Applying the column-wise softmax function across the key indices $k \in [P]$ yields the attention weights $(\mathbf{A}_2^1)_{k,j}$. Since the normalization denominator is $S_j = \sum_{l=1}^P \exp(s_{l,j})$, we have

$$(\mathbf{A}_2^1)_{k,j} = \frac{\exp(s_{k,j})}{\sum_{l=1}^P \exp(s_{l,j})} = \begin{cases} \frac{\exp(\tilde{T}_k(\mathbf{x}))}{\sum_{l=1}^P \exp(\tilde{T}_l(\mathbf{x}))} = \tilde{\beta}_k(\mathbf{x}), & j = 1, \\ \frac{\exp(0)}{\sum_{l=1}^P \exp(0)} = \frac{1}{P}, & j \neq 1. \end{cases}$$

The aggregated scalar output for the j -th token is

$$\mathbf{H}_{:,j} = \sum_{k=1}^P (\mathbf{A}_2^1)_{k,j} (\mathbf{V}_2^1 \mathbf{Z}_1)_{:,k} = \begin{cases} \sum_{k=1}^P \tilde{\beta}_k(\mathbf{x}) \tilde{R}_k(\mathbf{x}) = \hat{g}_T(\mathbf{x}), & j = 1, \\ \frac{1}{P} \sum_{k=1}^P \tilde{R}_k(\mathbf{x}) := \tilde{R}(\mathbf{x}), & j \neq 1. \end{cases}$$

We define the output projection matrix $\mathbf{W}^O \in \mathbb{R}^{D \times 1}$ as $\mathbf{W}^O = \mathbf{e}_1$. The output columns are

$$(\widehat{\mathbf{Z}}_2)_{:,j} = \mathbf{W}^O \mathbf{H}_{:,j} = \begin{cases} \widehat{g}_T(\mathbf{x}) \mathbf{e}_1, & j = 1, \\ \widetilde{R}(\mathbf{x}) \mathbf{e}_1, & j \neq 1. \end{cases}$$

Since all entries in the projection matrices are canonical basis elements, the maximum parameter magnitude is bounded by $M_{\mathcal{A}_2} = 1$. Thus we complete the proof. \square

B Proof of approximation results in Theorems 1 and 3

This section contains the comprehensive proofs for our main approximation guarantees. By assembling the foundational Transformer construction lemmas established in Subsection A.3, we construct the full architectures required for the target functions. We need the following lemma from Corollary A.7 in [11].

Lemma 8. *For any $\boldsymbol{\theta}, \boldsymbol{\theta}' \in \mathbb{R}^d$, we have*

$$\|\text{Softmax}(\boldsymbol{\theta}) - \text{Softmax}(\boldsymbol{\theta}')\|_1 \leq 2\|\boldsymbol{\theta} - \boldsymbol{\theta}'\|_\infty.$$

B.1 Approximation proof in Theorem 1

We provide the detailed construction and error bound analysis for Theorem 1. This formally establishes the uniform ε -approximation error for Hölder continuous functions defined on Euclidean domains.

Proof of Theorem 1. Applying Lemma 1 with target accuracy $\varepsilon/2$ yields P centers $\{\mathbf{c}_j\}_{j=1}^P \subset [0, 1]^d$ with

$$P \leq (\sqrt{d}(4C_H)^{1/\alpha})^d (\varepsilon/2)^{-\frac{d}{\alpha}} = C_P \varepsilon^{-\frac{d}{\alpha}}, \quad \text{where } C_P = (\sqrt{d}(8C_H)^{1/\alpha})^d.$$

Define the target affine features $T_j(\mathbf{x}) := 2M_g \mathbf{c}_j^\top \mathbf{x} - M_g \|\mathbf{c}_j\|_2^2$ and $R_j(\mathbf{x}) := g(\mathbf{c}_j)$. The corresponding Softmax POU approximation is given by

$$\widehat{g}(\mathbf{x}) = \sum_{j=1}^P \beta_j(\mathbf{x}) g(\mathbf{c}_j) = \sum_{j=1}^P \frac{\exp(T_j(\mathbf{x}))}{\sum_{l=1}^P \exp(T_l(\mathbf{x}))} g(\mathbf{c}_j). \quad (8)$$

By Lemma 1, this approximation satisfies

$$\sup_{\mathbf{x} \in [0, 1]^d} |\widehat{g}(\mathbf{x}) - g(\mathbf{x})| \leq \varepsilon/2,$$

provided that

$$M_g = C_M \varepsilon^{-\frac{2}{\alpha}} \log \frac{2}{\varepsilon}, \quad \text{with } C_M = \frac{(8C_H)^{2/\alpha}}{3} \left(\log(4B(\sqrt{d}(4C_H)^{1/\alpha})^d) + \frac{d+\alpha}{\alpha} \right).$$

Furthermore, since $\mathbf{x}, \mathbf{c}_j \in [0, 1]^d$, the magnitudes of these target features are bounded by

$$B_T := \max_{j \in [P]} \|T_j\|_\infty \leq 2M_g \sup_{\mathbf{x} \in [0, 1]^d} |\mathbf{c}_j^\top \mathbf{x}| + M_g \|\mathbf{c}_j\|_2^2 \leq 3M_g d,$$

$$B_R := \max_{j \in [P]} \|R_j\|_\infty = \max_{j \in [P]} |g(\mathbf{c}_j)| \leq \|g\|_\infty \leq B.$$

Step 1: Transformer Construction. By Lemma 4, the input \mathbf{x} is mapped to the initial sequence matrix $\mathbf{Z}_0 = \mathcal{P}(\mathbf{x}) \in \mathbb{R}^{D \times P}$ structured as

$$\mathbf{Z}_0 = \begin{bmatrix} \mathbf{x} & \mathbf{0} & \cdots & \mathbf{0} \\ 1 & 0 & \cdots & 0 \\ 0 & 0 & \cdots & 0 \\ \sin(\theta_1) & \sin(\theta_2) & \cdots & \sin(\theta_P) \\ \cos(\theta_1) & \cos(\theta_2) & \cdots & \cos(\theta_P) \end{bmatrix}.$$

For Encoder Block 1, applying the MHA layer \mathcal{A}_1 from Lemma 5 yields $\widehat{\mathbf{Z}}_1 = \mathcal{A}_1(\mathbf{Z}_0) \in \mathbb{R}^{D \times P}$, where the j -th column evaluates to

$$(\widehat{\mathbf{Z}}_1)_{:,j} = [\widetilde{T}_j(\mathbf{x}), \widetilde{g}(\mathbf{c}_j), \mathbf{0}_{d-1}^\top, \widetilde{I}_j, \lambda(M) \sin(\theta_j), \lambda(M) \cos(\theta_j)]^\top, \quad \forall j \in [P],$$

where $\widetilde{I}_1 = \eta(M) := \frac{e^M}{\sum_{l=1}^P e^{M \cos(\theta_l)}}$, and

$$0 \leq 1 - \widetilde{I}_1 = 1 - \eta(M) \leq (P-1)e^{-cM}, \quad \text{for } j = 1,$$

$$0 \leq \widetilde{I}_j \leq e^{-cM}, \quad \text{for } j \neq 1.$$

The features $\widetilde{T}_j(\mathbf{x})$ and $\widetilde{g}(\mathbf{c}_j)$ approximate the target affine expressions with bounded errors

$$|\widetilde{T}_j(\mathbf{x}) - T_j(\mathbf{x})| \leq 3(P-1)M_g d e^{-cM},$$

$$|\widetilde{g}(\mathbf{c}_j) - g(\mathbf{c}_j)| \leq (P-1)B e^{-cM}.$$

Next, applying the FFN layer \mathcal{F}_1 from Lemma 6 restores the structural components, yielding $\mathbf{Z}_1 = \mathcal{F}_1(\widehat{\mathbf{Z}}_1)$ with columns

$$(\mathbf{Z}_1)_{:,j} = [\widetilde{T}_j(\mathbf{x}), \widetilde{g}(\mathbf{c}_j), \mathbf{0}_{d-1}^\top, \delta_{j,1}, \sin(\theta_j), \cos(\theta_j)]^\top, \quad \forall j \in [P].$$

For Encoder Block 2, applying the MHA layer \mathcal{A}_2 from Lemma 7 that computes attention scores over $\widetilde{T}_j(\mathbf{x})$ and aggregates local function approximations $\widetilde{g}(\mathbf{c}_j)$. The output $\widehat{\mathbf{Z}}_2 = \mathcal{A}_2(\mathbf{Z}_1)$ has its first column to be

$$(\widehat{\mathbf{Z}}_2)_{:,1} = [\widehat{g}_T(\mathbf{x}), \mathbf{0}_{D-1}^\top]^\top = \widehat{g}_T(\mathbf{x}) \mathbf{e}_1,$$

where

$$\widehat{g}_T(\mathbf{x}) = \sum_{j=1}^P \widetilde{\beta}_j(\mathbf{x}) \widetilde{g}(\mathbf{c}_j), \quad \widetilde{\beta}_j(\mathbf{x}) = \frac{\exp(\widetilde{T}_j(\mathbf{x}))}{\sum_{l=1}^P \exp(\widetilde{T}_l(\mathbf{x}))},$$

all other columns ($k \neq 1$) evaluate to constant vectors $\widetilde{R}(\mathbf{x}) \mathbf{e}_1$, where $\widetilde{R}(\mathbf{x}) = \frac{1}{P} \sum_{j=1}^P \widetilde{R}_j(\mathbf{x})$. The second point-wise FFN layer \mathcal{F}_2 preserves this output via an exact identity mapping, exploiting the ReLU property $x = \sigma(x) - \sigma(-x)$. Specifically, we set the hidden dimension $d_{\text{ff}} = 2D = 2d + 8$,

and configure the weights ($\mathbf{W}_1 \in \mathbb{R}^{2D \times D}$, $\mathbf{W}_2 \in \mathbb{R}^{D \times 2D}$) and biases ($\mathbf{b}_1 \in \mathbb{R}^{2D}$, $\mathbf{b}_2 \in \mathbb{R}^D$) as

$$\mathbf{W}_1 = \begin{bmatrix} \mathbf{I}_D \\ -\mathbf{I}_D \end{bmatrix}, \quad \mathbf{b}_1 = \mathbf{0}_{2D}, \quad \mathbf{W}_2 = [\mathbf{I}_D \quad -\mathbf{I}_D], \quad \mathbf{b}_2 = \mathbf{0}_D.$$

This yields $\mathbf{Z}_2 = \mathcal{F}_2(\widehat{\mathbf{Z}}_2) = \mathbf{W}_2 \sigma(\mathbf{W}_1 \widehat{\mathbf{Z}}_2) = \widehat{\mathbf{Z}}_2$. Finally, the scalar regression output is then obtained by reading out the relevant components of \mathbf{Z}_2 , via a linear affine mapping $\mathbf{c}_3^\top \text{vec}(\mathbf{Z}_2)$, where setting $\mathbf{c}_3 = [1, 0, \dots, 0]^\top \in \mathbb{R}^{DP}$ explicitly extracts $\widehat{g}_T(\mathbf{x})$.

Step 2: Error Bound Analysis. According to Lemma 8,

$$\sum_{j=1}^P |\widetilde{\beta}_j(\mathbf{x}) - \beta_j(\mathbf{x})| \leq 2 \max_{j \in [P]} |\widetilde{T}_j(\mathbf{x}) - T_j(\mathbf{x})| \leq 6(P-1)M_g d e^{-cM}.$$

It follows that the approximation error of the Transformer is bounded by

$$\begin{aligned} |\widehat{g}_T(\mathbf{x}) - \widehat{g}(\mathbf{x})| &= \left| \sum_{j=1}^P \widetilde{\beta}_j(\mathbf{x}) \widetilde{g}(\mathbf{c}_j) - \sum_{j=1}^P \beta_j(\mathbf{x}) g(\mathbf{c}_j) \right| \\ &\leq \sum_{j=1}^P \widetilde{\beta}_j(\mathbf{x}) |\widetilde{g}(\mathbf{c}_j) - g(\mathbf{c}_j)| + \sum_{j=1}^P |\widetilde{\beta}_j(\mathbf{x}) - \beta_j(\mathbf{x})| |g(\mathbf{c}_j)| \\ &\leq (P-1)B e^{-cM} + 6(P-1)M_g d e^{-cM} \cdot B \\ &= (P-1)B(1 + 6M_g d) e^{-cM}. \end{aligned}$$

By setting the scaling factor $M = \frac{1}{c} \log \left(\frac{2(P-1)B(1+6M_g d)}{\varepsilon} \right)$, the implementation error is strictly bounded by $\varepsilon/2$. Combining this with the approximation error of the ideal Softmax POU, the triangle inequality yields

$$\sup_{\mathbf{x} \in [0,1]^d} |\widehat{g}_T(\mathbf{x}) - g(\mathbf{x})| \leq \sup_{\mathbf{x} \in [0,1]^d} |\widehat{g}_T(\mathbf{x}) - \widehat{g}(\mathbf{x})| + \sup_{\mathbf{x} \in [0,1]^d} |\widehat{g}(\mathbf{x}) - g(\mathbf{x})| \leq \frac{\varepsilon}{2} + \frac{\varepsilon}{2} = \varepsilon.$$

Step 3: Parameter Complexity. We count the total architectural (dense) parameters \mathcal{N}_{total} based on the embedding dimension $D = d + 4$:

- **Pre-processing:** Affine mapping $\mathbb{R}^d \rightarrow \mathbb{R}^{D \times P}$ has $D(P + d + 1)$ parameters.
- **MHA₁:** $H = P + 2$ heads with $d_k = d_v = 2$ have $8(P + 2)D$ parameters.
- **FFN₁:** Hidden dimension $2D$ has $4D^2 + 3D = 4d^2 + 35d + 76$ parameters.
- **MHA₂:** $H = 1$ head with $d_k = d_v = 1$ has $4D$ parameters.
- **FFN₂:** Hidden dimension $2D$ has $4D^2 + 3D = 4d^2 + 35d + 76$ parameters.
- **Readout:** Linear projection over $\text{vec}(\mathbf{Z}_2)$ has DP parameters.

Summing these contributions yields:

$$\begin{aligned} \mathcal{N}_{total} &= D(P + d + 1) + 8D(P + 2) + (4d^2 + 35d + 76) + 4D + (4d^2 + 35d + 76) + DP \\ &= 10P(d + 4) + 9d^2 + 95d + 236. \end{aligned}$$

Since $P \leq C_P \varepsilon^{-d/\alpha}$ and $\varepsilon \leq 1/e \implies \varepsilon^{-d/\alpha} > 1$, we obtain

$$\mathcal{N}_{total} \leq [10(d+4)C_P + 9d^2 + 95d + 236] \varepsilon^{-d/\alpha} := C_N \varepsilon^{-d/\alpha}.$$

Step 4: Parameter Bounds. According to our construction, to bound the global parameter magnitude $M_{max} \leq \max\{1, M, \frac{1}{1-2Pe^{-cM}}, (1+(P-1)e^{-cM})B_{\mathcal{A}_1}\}$, we first bound M . Since $P \geq 2$, we have $\sin(\pi/P) \geq 2/P$, yielding

$$\frac{1}{c} = \frac{1}{2 \sin^2(\pi/P)} \leq \frac{P^2}{8} \leq \frac{C_P^2}{8} \varepsilon^{-2d/\alpha}.$$

For $\varepsilon \leq 1/e$, substituting $P \leq C_P \varepsilon^{-d/\alpha}$ and $M_g \leq C_M \varepsilon^{-2/\alpha} \log(2/\varepsilon)$ yields

$$\log\left(\frac{2(P-1)B(1+6M_g d)}{\varepsilon}\right) \leq \log\left(\frac{2C_P B(1+6dC_M)}{\varepsilon^{(d+2+\alpha)/\alpha}} \log \frac{2}{\varepsilon}\right) \leq C_{log} \log \frac{1}{\varepsilon},$$

where $C_{log} = |\log(4C_P B(1+6dC_M))| + \frac{d+2+\alpha}{\alpha} + 2$. It follows that

$$M = \frac{1}{c} \log\left(\frac{4(P-1)B(1+6M_g d)}{\varepsilon}\right) \leq C_{mag} \varepsilon^{-2d/\alpha} \log \frac{1}{\varepsilon}, \quad \text{where } C_{mag} = \frac{C_P^2 C_{log}}{8}.$$

Next, by definition $e^{-cM} = \frac{\varepsilon}{2(P-1)B(1+6M_g d)}$. Since $1+6M_g d > 2 \geq \frac{P}{P-1}$, we have

$$2Pe^{-cM} = \frac{2P}{P-1} \frac{\varepsilon}{2B(1+6M_g d)} \leq \frac{\varepsilon}{B} \implies \frac{1}{1-2Pe^{-cM}} \leq \frac{1}{1-\frac{\varepsilon}{B}} \leq \frac{1}{1-\frac{1}{eB}}.$$

Moreover, since $B_{\mathcal{A}_1} \leq \max\{3M_g d, B, 1\} \leq C_B \varepsilon^{-2/\alpha} \log(2/\varepsilon)$ with $C_B = \max\{3dC_M, B, 1\}$. Similarly bounding $(P-1)e^{-cM} \leq \frac{\varepsilon}{2B}$, it follows that

$$(1+(P-1)e^{-cM})B_{\mathcal{A}_1} \leq \left(1 + \frac{\varepsilon}{2B}\right) C_B \varepsilon^{-2/\alpha} \log \frac{2}{\varepsilon} \leq 2\left(1 + \frac{1}{2eB}\right) C_B \varepsilon^{-2d/\alpha} \log \frac{1}{\varepsilon}.$$

Consequently, the global parameter magnitude satisfies

$$\begin{aligned} M_{max} &\leq \max\left\{\frac{1}{1-\frac{1}{eB}}, C_{mag} \varepsilon^{-2d/\alpha} \log \frac{1}{\varepsilon}, 2\left(1 + \frac{1}{2eB}\right) C_B \varepsilon^{-2d/\alpha} \log \frac{1}{\varepsilon}\right\} \\ &\leq \max\left\{\frac{1}{1-\frac{1}{eB}}, C_{mag}, 2\left(1 + \frac{1}{2eB}\right) C_B\right\} \varepsilon^{-2d/\alpha} \log \frac{1}{\varepsilon} := \tilde{C}_{mag} \varepsilon^{-2d/\alpha} \log \frac{1}{\varepsilon}, \end{aligned} \quad (9)$$

This completes the proof. \square

B.2 Approximation proof in Theorem 3

In this subsection, we prove Theorem 3 by adapting our constructive Transformer framework in Subsection B.1 to Riemannian manifolds.

Proof of Theorem 3. Applying Lemma 3 (Softmax POU Approximation on Manifolds) with target accuracy $\varepsilon/2$ yields $P = C_g \leq C_P \varepsilon^{-d/\alpha}$ centers $\{\mathbf{c}_j\}_{j=1}^P \subset \mathcal{M}$, where $C_P = C_{\mathcal{M}}(16C_H)^{d/\alpha}$. Define the target affine features $T_j(\mathbf{x}) := 2M_g \mathbf{c}_j^\top \mathbf{x} - M_g \|\mathbf{c}_j\|_2^2$ and $R_j(\mathbf{x}) := g(\mathbf{c}_j)$. The corresponding

Softmax POU approximation is given by

$$\widehat{g}(\mathbf{x}) = \sum_{j=1}^P \beta_j(\mathbf{x})g(\mathbf{c}_j) = \sum_{j=1}^P \frac{\exp(T_j(\mathbf{x}))}{\sum_{l=1}^P \exp(T_l(\mathbf{x}))} g(\mathbf{c}_j).$$

By Lemma 3, this achieves

$$\sup_{\mathbf{x} \in \mathcal{M}} |\widehat{g}(\mathbf{x}) - g(\mathbf{x})| \leq \varepsilon/2$$

provided that

$$M_g = C_M \varepsilon^{-2/\alpha} \log \frac{2}{\varepsilon}, \quad \text{where } C_M = \frac{(16C_H)^{2/\alpha}}{3} \left(\log(4BC_P) + \frac{d + \alpha}{\alpha} \right).$$

Since $\mathbf{x}, \mathbf{c}_j \in \mathcal{M} \subseteq [0, 1]^{\bar{d}}$, the magnitudes of target features are bounded by $B_T := \max_{j \in [P]} \|T_j\|_\infty \leq 3M_g \bar{d}$ and $B_R := \max_{j \in [P]} \|R_j\|_\infty \leq B$.

Step 1: Transformer Construction. Following the exact architecture construction as in the proof of Theorem 1, but operating on the ambient dimension \bar{d} instead of d , the pre-processing layer maps the input $\mathbf{x} \in \mathbb{R}^{\bar{d}}$ to $\mathbf{Z}_0 \in \mathbb{R}^{D \times P}$ using the embedding dimension $D = \bar{d} + 4$. The first encoder block (MHA₁ and FFN₁) achieves local features and restores the structural components to exact canonical forms, yielding $\mathbf{Z}_1 \in \mathbb{R}^{D \times P}$ with columns

$$(\mathbf{Z}_1)_{:,j} = [\widetilde{T}_j(\mathbf{x}), \widetilde{g}(\mathbf{c}_j), \mathbf{0}_{\bar{d}-1}^\top, \delta_{j,1}, \sin(\theta_j), \cos(\theta_j)]^\top, \quad \forall j \in [P].$$

The local features approximate the targets with bounded errors

$$\begin{aligned} |\widetilde{T}_j(\mathbf{x}) - T_j(\mathbf{x})| &\leq 3(P-1)M_g \bar{d} e^{-cM}, \\ |\widetilde{g}(\mathbf{c}_j) - g(\mathbf{c}_j)| &\leq (P-1)B e^{-cM}. \end{aligned}$$

The second encoder block (MHA₂ and FFN₂) computes the softmax attention and aggregates the values, and the readout extracts

$$\widehat{g}_T(\mathbf{x}) = \sum_{j=1}^P \widetilde{\beta}_j(\mathbf{x}) \widetilde{g}(\mathbf{c}_j), \quad \widetilde{\beta}_j(\mathbf{x}) = \frac{\exp(\widetilde{T}_j(\mathbf{x}))}{\sum_{l=1}^P \exp(\widetilde{T}_l(\mathbf{x}))}.$$

Step 2: Error Bound Analysis. By the softmax Lipschitz property Lemma 8,

$$\sum_{j=1}^P |\widetilde{\beta}_j(\mathbf{x}) - \beta_j(\mathbf{x})| \leq 2 \max_j |\widetilde{T}_j(\mathbf{x}) - T_j(\mathbf{x})| \leq 6(P-1)M_g \bar{d} e^{-cM}.$$

The network approximation error is bounded by

$$\begin{aligned} |\widehat{g}_T(\mathbf{x}) - \widehat{g}(\mathbf{x})| &\leq \sum_{j=1}^P \widetilde{\beta}_j(\mathbf{x}) |\widetilde{g}(\mathbf{c}_j) - g(\mathbf{c}_j)| + \sum_{j=1}^P |\widetilde{\beta}_j(\mathbf{x}) - \beta_j(\mathbf{x})| |g(\mathbf{c}_j)| \\ &\leq (P-1)B e^{-cM} + 6(P-1)M_g \bar{d} e^{-cM} B \\ &= (P-1)B(1 + 6M_g \bar{d}) e^{-cM}. \end{aligned}$$

Setting the MHA scaling factor $M = \frac{1}{c} \log \left(\frac{2(P-1)B(1+6M_g\bar{d})}{\varepsilon} \right)$ bounds this implementation error by $\varepsilon/2$. The triangle inequality yields the target bound

$$\sup_{\mathbf{x} \in \mathcal{M}} |\widehat{g}_T(\mathbf{x}) - g(\mathbf{x})| \leq \sup_{\mathbf{x} \in \mathcal{M}} |\widehat{g}_T(\mathbf{x}) - \widehat{g}(\mathbf{x})| + \sup_{\mathbf{x} \in \mathcal{M}} |\widehat{g}(\mathbf{x}) - g(\mathbf{x})| \leq \frac{\varepsilon}{2} + \frac{\varepsilon}{2} = \varepsilon.$$

Step 3: Parameter Complexity. With the embedding dimension $D = \bar{d} + 4$, similarly as the Proof of Theorem 1, the total number of dense architectural parameters \mathcal{N}_{total} is

$$\begin{aligned} \mathcal{N}_{total} &= D(P + \bar{d} + 1) + 8D(P + 2) + (4\bar{d}^2 + 35\bar{d} + 76) + 4D \\ &\quad + (4\bar{d}^2 + 35\bar{d} + 76) + DP \\ &= 10P(\bar{d} + 4) + 9\bar{d}^2 + 95\bar{d} + 236. \end{aligned}$$

Since $P \leq C_P \varepsilon^{-d/\alpha}$ and $\varepsilon \leq 1/e \implies \varepsilon^{-d/\alpha} > 1$, we obtain

$$\mathcal{N}_{total} \leq [10(\bar{d} + 4)C_P + 9\bar{d}^2 + 95\bar{d} + 236] \varepsilon^{-d/\alpha} := C_N \varepsilon^{-d/\alpha}.$$

Notice that the parameter complexity scales strictly with $\varepsilon^{-d/\alpha}$, successfully bypassing the ambient dimension \bar{d} in the exponent.

Step 4: Parameter Bounds. To bound the global parameter magnitude that $M_{max} \leq \max \left\{ 1, M, \frac{1}{1-2Pe^{-cM}}, (1 + (P-1)e^{-cM})B_{A_1} \right\}$, we explicitly substitute $P \leq C_P \varepsilon^{-d/\alpha}$ and $M_g \leq C_M \varepsilon^{-2/\alpha} \log(2/\varepsilon)$ for $\varepsilon \leq 1/e$. First, we bound M , since

$$\frac{1}{c} = \frac{1}{2 \sin^2(\pi/P)} \leq \frac{P^2}{8} \leq \frac{C_P^2}{8} \varepsilon^{-2d/\alpha},$$

and

$$\begin{aligned} \log \left(\frac{2(P-1)B(1+6M_g\bar{d})}{\varepsilon} \right) &\leq \log \left(\frac{2C_P B \varepsilon^{-d/\alpha} (1 + 6\bar{d} C_M \varepsilon^{-2/\alpha} \log(2/\varepsilon))}{\varepsilon} \right) \\ &\leq \log \left(\frac{2C_P B (1 + 6\bar{d} C_M)}{\varepsilon^{(d+2+\alpha)/\alpha}} \log \frac{2}{\varepsilon} \right) \leq C_{log} \log \frac{1}{\varepsilon}, \end{aligned}$$

where $C_{log} = \left| \log(2C_P B (1 + 6\bar{d} C_M)) \right| + \frac{d+2+\alpha}{\alpha} + 2$. It follows that

$$M = \frac{1}{c} \log \left(\frac{2(P-1)B(1+6M_g\bar{d})}{\varepsilon} \right) \leq C_{mag} \varepsilon^{-2d/\alpha} \log \frac{1}{\varepsilon}, \quad \text{where } C_{mag} = \frac{C_P^2 C_{log}}{8}.$$

Next, by definition $e^{-cM} = \frac{\varepsilon}{2(P-1)B(1+6M_g\bar{d})}$. Since $1 + 6M_g\bar{d} > 2 \geq \frac{P}{P-1}$, we bound the denominator term purely in ε :

$$2Pe^{-cM} = \frac{2P}{P-1} \frac{\varepsilon}{2B(1+6M_g\bar{d})} \leq \frac{\varepsilon}{B} \implies \frac{1}{1-2Pe^{-cM}} \leq \frac{1}{1-\frac{1}{eB}}.$$

For the feature magnitude, substituting M_g yields $B_{A_1} \leq \max\{3M_g\bar{d}, B, 1\} \leq C_B \varepsilon^{-2/\alpha} \log(2/\varepsilon)$

with $C_B = \max\{3\bar{d}C_M, B, 1\}$. Similarly bounding $(P-1)e^{-cM} \leq \frac{\varepsilon}{2B}$, it follows that

$$(1 + (P-1)e^{-cM})B_{\mathcal{A}_1} \leq \left(1 + \frac{\varepsilon}{2B}\right)C_B\varepsilon^{-2/\alpha} \log \frac{2}{\varepsilon} \leq 2\left(1 + \frac{1}{2eB}\right)C_B\varepsilon^{-2d/\alpha} \log \frac{1}{\varepsilon}.$$

Consequently, the global parameter magnitude satisfies

$$\begin{aligned} M_{max} &\leq \max \left\{ \frac{1}{1 - \frac{1}{eB}}, C_{mag}\varepsilon^{-2d/\alpha} \log \frac{1}{\varepsilon}, 2\left(1 + \frac{1}{2eB}\right)C_B\varepsilon^{-2d/\alpha} \log \frac{1}{\varepsilon} \right\} \\ &\leq \max \left\{ \frac{1}{1 - \frac{1}{eB}}, C_{mag}, 2\left(1 + \frac{1}{2eB}\right)C_B \right\} \varepsilon^{-2d/\alpha} \log \frac{1}{\varepsilon} := \tilde{C}_{mag}\varepsilon^{-2d/\alpha} \log \frac{1}{\varepsilon}, \end{aligned} \quad (10)$$

This completes the proof. \square

C Proof of generalization results in Theorems 2 and 4

This final section details the proofs for the statistical generalization bounds of the empirical risk minimizer. We calculate the capacity of the hypothesis space and leverage it to derive near minimax-optimal learning rates.

C.1 Bounding the covering number

We first rigorously bound the covering number of our constructed Transformer hypothesis space in the following lemma. This provides the essential capacity measure necessary for controlling the statistical estimation error.

Lemma 9 (Covering Number of the Transformer Class). *Let \mathcal{T} be the class of Transformer networks defined in Theorem 1 (Theorem 3) with $L = 2$, sequence length P , embedding dimension $D = d + 4$ ($D = \bar{d} + 4$), and parameter magnitude bounded by $M_{max} \geq 1$. For any $\eta \in (0, 1]$, the covering number of \mathcal{T} satisfies*

$$\log \mathcal{N}(\eta, \mathcal{T}, \|\cdot\|_\infty) \leq \mathcal{N}_{total} \log \left(\frac{1224256P^4 D^{22} M_{max}^{26}}{\eta} \right),$$

where \mathcal{N}_{total} is the total number of parameters.

Proof of Lemma 9. In the proof, we consider the class of Transformer networks defined in Theorem 3, the one defined in Theorem 1 follows the same result. Let $\hat{g}_T(\mathbf{x}; \boldsymbol{\theta})$ and $\tilde{g}_T(\mathbf{x}; \tilde{\boldsymbol{\theta}})$ be two Transformer networks in \mathcal{T} parameterized by $\boldsymbol{\theta}$ and $\tilde{\boldsymbol{\theta}}$ respectively, where $\|\boldsymbol{\theta}\|_\infty, \|\tilde{\boldsymbol{\theta}}\|_\infty \leq M_{max}$. Assume the parameter difference is bounded by $\|\boldsymbol{\theta} - \tilde{\boldsymbol{\theta}}\|_\infty \leq \delta$. We aim to bound the output difference $\|\hat{g}_T - \tilde{g}_T\|_\infty$ with respect to δ .

Step 1: Pre-processing and First Encoder Block. For any input $\mathbf{x} \in \mathcal{M} \subseteq [0, 1]^{\bar{d}}$, the pre-processing layer maps \mathbf{x} to the initial embedding matrix $\mathbf{Z}_0 \in \mathbb{R}^{D \times P}$ via

$$\mathbf{Z}_0 = \mathcal{P}(\mathbf{x}) = (\mathbf{W}_E \mathbf{x} + \mathbf{b}_E) \mathbf{e}_1^\top + \mathbf{P},$$

where $\mathbf{W}_E \in \mathbb{R}^{D \times \bar{d}}$, $\mathbf{b}_E \in \mathbb{R}^D$, and $\mathbf{P} \in \mathbb{R}^{D \times P}$ are parameterized by $\boldsymbol{\theta}$. Since $D = \bar{d} + 4$, $\|\mathbf{x}\|_\infty \leq 1$, and all trainable parameters are bounded by M_{max} , we calculate the bound for the magnitude

$r_0 := \|\mathbf{Z}_0\|_{max}$ and the difference $\|\mathbf{Z}_0 - \tilde{\mathbf{Z}}_0\|_{max}$ as

$$\begin{aligned} r_0 &= \|(\mathbf{W}_E \mathbf{x} + \mathbf{b}_E) \mathbf{e}_1^\top + \mathbf{P}\|_{max} \leq \bar{d} \|\mathbf{W}_E\|_{max} \|\mathbf{x}\|_\infty + \|\mathbf{b}_E\|_{max} + \|\mathbf{P}\|_{max} \leq DM_{max}, \\ \|\mathbf{Z}_0 - \tilde{\mathbf{Z}}_0\|_{max} &= \|((\mathbf{W}_E - \tilde{\mathbf{W}}_E) \mathbf{x} + (\mathbf{b}_E - \tilde{\mathbf{b}}_E)) \mathbf{e}_1^\top + (\mathbf{P} - \tilde{\mathbf{P}})\|_{max} \leq \bar{d} \delta + \delta + \delta \leq D\delta. \end{aligned}$$

Let \mathcal{A}_1 and \mathcal{F}_1 denote the MHA and FFN mappings in the first block. We first consider the concatenated output of the H_1 attention heads before the final projection, denoted as $\mathcal{H}_1(\mathbf{Z}_0) \in \mathbb{R}^{(H_1 d_v) \times P}$. For a single attention head $h \in [H_1]$, let $\mathbf{E}_1^h = \mathbf{Z}_0^\top (\mathbf{K}_1^h)^\top \mathbf{Q}_1^h \mathbf{Z}_0 \in \mathbb{R}^{P \times P}$ be the pre-softmax score matrix, $\mathbf{A}_1^h = \text{Softmax}(\mathbf{E}_1^h) \in \mathbb{R}^{P \times P}$ be the attention probability matrix, and head $_1^h = \mathbf{V}_1^h \mathbf{Z}_0 \mathbf{A}_1^h \in \mathbb{R}^{d_v \times P}$ be the head output. By Theorem 3, the inner dimensions are $d_k = d_v = 2$. We decouple the difference into a parameter error and an input error

$$\|\mathcal{H}_1(\mathbf{Z}_0) - \tilde{\mathcal{H}}_1(\tilde{\mathbf{Z}}_0)\|_{max} \leq \underbrace{\|\mathcal{H}_1(\mathbf{Z}_0) - \tilde{\mathcal{H}}_1(\mathbf{Z}_0)\|_{max}}_{\text{(I) Parameter Error}} + \underbrace{\|\tilde{\mathcal{H}}_1(\mathbf{Z}_0) - \tilde{\mathcal{H}}_1(\tilde{\mathbf{Z}}_0)\|_{max}}_{\text{(II) Input Error}}.$$

(I) *Parameter Error*: Fixing the input \mathbf{Z}_0 , for the pre-softmax matrix \mathbf{E}_1^h , we have

$$\begin{aligned} \|(\mathbf{K}_1^h)^\top \mathbf{Q}_1^h - (\tilde{\mathbf{K}}_1^h)^\top \tilde{\mathbf{Q}}_1^h\|_{max} &\leq d_k \|\mathbf{K}_1^h\|_{max} \|\mathbf{Q}_1^h - \tilde{\mathbf{Q}}_1^h\|_{max} + d_k \|\mathbf{K}_1^h - \tilde{\mathbf{K}}_1^h\|_{max} \|\tilde{\mathbf{Q}}_1^h\|_{max} \\ &\leq 2d_k M_{max} \delta \leq 4M_{max} \delta, \\ \|\mathbf{E}_1^h - \tilde{\mathbf{E}}_1^h\|_{max} &= \|\mathbf{Z}_0^\top ((\mathbf{K}_1^h)^\top \mathbf{Q}_1^h - (\tilde{\mathbf{K}}_1^h)^\top \tilde{\mathbf{Q}}_1^h) \mathbf{Z}_0\|_{max} \\ &\leq D^2 \|\mathbf{Z}_0\|_{max}^2 \|(\mathbf{K}_1^h)^\top \mathbf{Q}_1^h - (\tilde{\mathbf{K}}_1^h)^\top \tilde{\mathbf{Q}}_1^h\|_{max} \leq 4D^2 r_0^2 M_{max} \delta. \end{aligned}$$

By Lemma 8, for each column $j \in [P]$,

$$\|(\mathbf{A}_1^h)_{:,j} - (\tilde{\mathbf{A}}_1^h)_{:,j}\|_1 \leq 2 \|(\mathbf{E}_1^h)_{:,j} - (\tilde{\mathbf{E}}_1^h)_{:,j}\|_\infty \leq 2 \|\mathbf{E}_1^h - \tilde{\mathbf{E}}_1^h\|_{max} \leq 8D^2 r_0^2 M_{max} \delta.$$

Since $\|(\mathbf{A}_1^h)_{:,j}\|_1 = 1$, $\|\mathbf{Z}_0 \mathbf{A}_1^h\|_{max} \leq \|\mathbf{Z}_0\|_{max} \leq r_0$, it follows that

$$\begin{aligned} &\|\text{head}_1^h - \tilde{\text{head}}_1^h\|_{max} \\ &= \|(\mathbf{V}_1^h - \tilde{\mathbf{V}}_1^h) \mathbf{Z}_0 \mathbf{A}_1^h + \tilde{\mathbf{V}}_1^h \mathbf{Z}_0 (\mathbf{A}_1^h - \tilde{\mathbf{A}}_1^h)\|_{max} \\ &\leq D \|\mathbf{V}_1^h - \tilde{\mathbf{V}}_1^h\|_{max} \|\mathbf{Z}_0 \mathbf{A}_1^h\|_{max} + \|\tilde{\mathbf{V}}_1^h \mathbf{Z}_0\|_{max} \max_{j \in [P]} \|(\mathbf{A}_1^h)_{:,j} - (\tilde{\mathbf{A}}_1^h)_{:,j}\|_1 \\ &\leq D\delta r_0 + (DM_{max} r_0) (8D^2 r_0^2 M_{max} \delta) \\ &\leq 9D^3 M_{max}^2 r_0^3 \delta. \end{aligned}$$

Since $\mathcal{H}_1(\mathbf{Z}_0)$ concatenates all H_1 heads, we have

$$(I) \leq 9D^3 M_{max}^2 r_0^3 \delta.$$

(II) *Input Error*: Fixing parameters $\tilde{\theta}$, We have

$$\begin{aligned}
& \|\mathbf{Z}_0^\top (\tilde{\mathbf{K}}_1^h)^\top \tilde{\mathbf{Q}}_1^h \mathbf{Z}_0 - \tilde{\mathbf{Z}}_0^\top (\tilde{\mathbf{K}}_1^h)^\top \tilde{\mathbf{Q}}_1^h \tilde{\mathbf{Z}}_0\|_{max} \\
& \leq \|(\mathbf{Z}_0 - \tilde{\mathbf{Z}}_0)^\top (\tilde{\mathbf{K}}_1^h)^\top \tilde{\mathbf{Q}}_1^h \mathbf{Z}_0\|_{max} + \|\tilde{\mathbf{Z}}_0^\top (\tilde{\mathbf{K}}_1^h)^\top \tilde{\mathbf{Q}}_1^h (\mathbf{Z}_0 - \tilde{\mathbf{Z}}_0)\|_{max} \\
& \leq 2D\|\mathbf{Z}_0 - \tilde{\mathbf{Z}}_0\|_{max} \|(\tilde{\mathbf{K}}_1^h)^\top \tilde{\mathbf{Q}}_1^h \mathbf{Z}_0\|_{max} \\
& \leq 2D\|\mathbf{Z}_0 - \tilde{\mathbf{Z}}_0\|_{max} (Dd_k M_{max}^2 r_0) \leq 4D^2 M_{max}^2 r_0 \|\mathbf{Z}_0 - \tilde{\mathbf{Z}}_0\|_{max}.
\end{aligned}$$

Notice that $\max_j \|(\mathbf{A}_1^h)_{:,j} - (\tilde{\mathbf{A}}_1^h)_{:,j}\|_1 \leq 8D^2 M_{max}^2 r_0 \|\mathbf{Z}_0 - \tilde{\mathbf{Z}}_0\|_{max}$. It follows that

$$\begin{aligned}
& \|\tilde{\mathbf{V}}_1^h \mathbf{Z}_0 \mathbf{A}_1^h - \tilde{\mathbf{V}}_1^h \tilde{\mathbf{Z}}_0 \tilde{\mathbf{A}}_1^h\|_{max} \\
& = \|\tilde{\mathbf{V}}_1^h (\mathbf{Z}_0 - \tilde{\mathbf{Z}}_0) \mathbf{A}_1^h + \tilde{\mathbf{V}}_1^h \tilde{\mathbf{Z}}_0 (\mathbf{A}_1^h - \tilde{\mathbf{A}}_1^h)\|_{max} \\
& \leq D\|\tilde{\mathbf{V}}_1^h\|_{max} \|\mathbf{Z}_0 - \tilde{\mathbf{Z}}_0\|_{max} + \|\tilde{\mathbf{V}}_1^h \tilde{\mathbf{Z}}_0\|_{max} \max_j \|(\mathbf{A}_1^h)_{:,j} - (\tilde{\mathbf{A}}_1^h)_{:,j}\|_1 \\
& \leq DM_{max} \|\mathbf{Z}_0 - \tilde{\mathbf{Z}}_0\|_{max} + (DM_{max} r_0) (8D^2 M_{max}^2 r_0 \|\mathbf{Z}_0 - \tilde{\mathbf{Z}}_0\|_{max}) \\
& \leq 9D^3 M_{max}^3 r_0^2 \|\mathbf{Z}_0 - \tilde{\mathbf{Z}}_0\|_{max}.
\end{aligned}$$

Thus, we have

$$(II) \leq 9D^3 M_{max}^3 r_0^2 \|\mathbf{Z}_0 - \tilde{\mathbf{Z}}_0\|_{max}.$$

Combining (I) and (II) with $r_0 \leq DM_{max}$ and $\|\mathbf{Z}_0 - \tilde{\mathbf{Z}}_0\|_{max} \leq D\delta$, we obtain

$$\begin{aligned}
\|\mathcal{H}_1(\mathbf{Z}_0) - \tilde{\mathcal{H}}_1(\tilde{\mathbf{Z}}_0)\|_{max} & \leq 9M_{max}^2 D^3 r_0^3 \delta + 9M_{max}^3 D^3 r_0^2 \|\mathbf{Z}_0 - \tilde{\mathbf{Z}}_0\|_{max} \\
& \leq 9M_{max}^2 D^3 (DM_{max})^3 \delta + 9M_{max}^3 D^3 (DM_{max})^2 (D\delta) \\
& \leq 18D^6 M_{max}^5 \delta.
\end{aligned}$$

Also, $\|\mathcal{H}_1(\mathbf{Z}_0)\|_{max} \leq DM_{max} r_0 \leq D^2 M_{max}^2$.

For $\mathcal{A}_1(\mathbf{Z}_0) = \mathbf{W}_1^O \mathcal{H}_1(\mathbf{Z}_0)$, since $H_1 d_v = (P+2) \times 2 \leq 6P$, we have

$$\begin{aligned}
\|\mathcal{A}_1(\mathbf{Z}_0) - \tilde{\mathcal{A}}_1(\tilde{\mathbf{Z}}_0)\|_{max} & \leq \|\mathbf{W}_1^O (\mathcal{H}_1(\mathbf{Z}_0) - \tilde{\mathcal{H}}_1(\tilde{\mathbf{Z}}_0))\|_{max} + \|(\mathbf{W}_1^O - \tilde{\mathbf{W}}_1^O) \tilde{\mathcal{H}}_1(\tilde{\mathbf{Z}}_0)\|_{max} \\
& \leq (6P)M_{max} \|\mathcal{H}_1(\mathbf{Z}_0) - \tilde{\mathcal{H}}_1(\tilde{\mathbf{Z}}_0)\|_{max} + (6P)\delta \|\tilde{\mathcal{H}}_1(\tilde{\mathbf{Z}}_0)\|_{max} \\
& \leq 6PM_{max} (18D^6 M_{max}^5 \delta) + 6P\delta (D^2 M_{max}^2) \\
& \leq 114PD^6 M_{max}^6 \delta,
\end{aligned}$$

and $\|\mathcal{A}_1(\mathbf{Z}_0)\|_{max} \leq (6P)M_{max} \|\mathcal{H}_1(\mathbf{Z}_0)\|_{max} \leq 6PD^2 M_{max}^3$.

For the FFN layer, let $\mathbf{Y}_1 = \sigma(\mathbf{W}_1^1 \mathcal{A}_1(\mathbf{Z}_0) + \mathbf{b}_1^1)$ and $\tilde{\mathbf{Y}}_1 = \sigma(\tilde{\mathbf{W}}_1^1 \tilde{\mathcal{A}}_1(\tilde{\mathbf{Z}}_0) + \tilde{\mathbf{b}}_1^1)$. Since σ is 1-Lipschitz, we have

$$\begin{aligned}
\|\mathbf{Y}_1 - \tilde{\mathbf{Y}}_1\|_{max} & \leq \|(\mathbf{W}_1^1 - \tilde{\mathbf{W}}_1^1) \mathcal{A}_1(\mathbf{Z}_0) + \tilde{\mathbf{W}}_1^1 (\mathcal{A}_1(\mathbf{Z}_0) - \tilde{\mathcal{A}}_1(\tilde{\mathbf{Z}}_0)) + (\mathbf{b}_1^1 - \tilde{\mathbf{b}}_1^1)\|_{max} \\
& \leq D\delta \|\mathcal{A}_1(\mathbf{Z}_0)\|_{max} + DM_{max} \|\mathcal{A}_1(\mathbf{Z}_0) - \tilde{\mathcal{A}}_1(\tilde{\mathbf{Z}}_0)\|_{max} + \delta \\
& \leq D\delta (6PD^2 M_{max}^3) + DM_{max} (114PD^6 M_{max}^6 \delta) + \delta \\
& \leq 121PD^7 M_{max}^7 \delta.
\end{aligned}$$

The magnitude is bounded by

$$\|\mathbf{Y}_1\|_{max} \leq DM_{max}\|\mathcal{A}_1(\mathbf{Z}_0)\|_{max} + M_{max} \leq DM_{max}(6PD^2M_{max}^3) + M_{max} \leq 7PD^3M_{max}^4.$$

Let $\mathbf{Z}_1 = \mathcal{F}_1(\mathcal{A}_1(\mathbf{Z}_0))$ and $\tilde{\mathbf{Z}}_1 = \tilde{\mathcal{F}}_1(\tilde{\mathcal{A}}_1(\tilde{\mathbf{Z}}_0))$. Since $d_{\text{ff}}^1 \leq 2D$, it follows that the output difference of the first encoder block is bounded by

$$\begin{aligned} \|\mathbf{Z}_1 - \tilde{\mathbf{Z}}_1\|_{max} &= \|(\mathbf{W}_1^2\mathbf{Y}_1 + \mathbf{b}_1^2) - (\tilde{\mathbf{W}}_1^2\tilde{\mathbf{Y}}_1 + \tilde{\mathbf{b}}_1^2)\|_{max} \\ &\leq \|(\mathbf{W}_1^2 - \tilde{\mathbf{W}}_1^2)\mathbf{Y}_1 + \tilde{\mathbf{W}}_1^2(\mathbf{Y}_1 - \tilde{\mathbf{Y}}_1) + (\mathbf{b}_1^2 - \tilde{\mathbf{b}}_1^2)\|_{max} \\ &\leq d_{\text{ff}}^1\delta(7PD^3M_{max}^4) + d_{\text{ff}}^1M_{max}(121PD^7M_{max}^7\delta) + \delta \\ &\leq 257PD^8M_{max}^8\delta. \end{aligned}$$

Its magnitude is bounded by

$$\begin{aligned} r_1 := \|\mathbf{Z}_1\|_{max} &\leq d_{\text{ff}}^1\|\mathbf{W}_1^2\|_{max}\|\mathbf{Y}\|_{max} + \|\mathbf{b}_1^2\|_{max} \\ &\leq 2DM_{max}(7PD^3M_{max}^4) + M_{max} \\ &\leq 15PD^4M_{max}^5. \end{aligned}$$

Step 2: Second Encoder Block. We recursively apply the same logic to the second block, utilizing \mathbf{Z}_1 as the input bounded by r_1 . For the second block, since $H_2 = 1$ and the inner dimensions are $d_k^2 = d_v^2 = 1$, the MHA bound simplifies. Adapting the derivation from Step 1 by substituting r_0 with r_1 , \mathbf{Z}_0 with \mathbf{Z}_1 , and updating the constants for $d_k = 1$, we have

$$\begin{aligned} \|\mathcal{H}_2(\mathbf{Z}_1) - \tilde{\mathcal{H}}_2(\tilde{\mathbf{Z}}_1)\|_{max} &\leq 5M_{max}^2D^3r_1^3\delta + 5M_{max}^3D^3r_1^2\|\mathbf{Z}_1 - \tilde{\mathbf{Z}}_1\|_{max} \\ &\leq 5M_{max}^2D^3(15PD^4M_{max}^5)^3\delta + 5M_{max}^3D^3(15PD^4M_{max}^5)^2(257PD^8M_{max}^8\delta) \\ &\leq 16875P^3D^{15}M_{max}^{17}\delta + 289125P^3D^{19}M_{max}^{21}\delta \\ &\leq 306000P^3D^{19}M_{max}^{21}\delta. \end{aligned}$$

Its magnitude is bounded by $\|\mathcal{H}_2(\mathbf{Z}_1)\|_{max} \leq DM_{max}r_1 \leq 15PD^5M_{max}^6$.

Applying the output projection $\mathbf{W}_2^O \in \mathbb{R}^{D \times 1}$ (since $H_2d_v^2 = 1$), we have

$$\begin{aligned} \|\mathcal{A}_2(\mathbf{Z}_1) - \tilde{\mathcal{A}}_2(\tilde{\mathbf{Z}}_1)\|_{max} &\leq 1 \cdot M_{max}\|\mathcal{H}_2(\mathbf{Z}_1) - \tilde{\mathcal{H}}_2(\tilde{\mathbf{Z}}_1)\|_{max} + 1 \cdot \delta\|\tilde{\mathcal{H}}_2(\tilde{\mathbf{Z}}_1)\|_{max} \\ &\leq M_{max}(306000P^3D^{19}M_{max}^{21}\delta) + \delta(15PD^5M_{max}^6) \\ &\leq 306015P^3D^{19}M_{max}^{22}\delta. \end{aligned}$$

The magnitude is $\|\mathcal{A}_2(\mathbf{Z}_1)\|_{max} \leq M_{max}\|\mathcal{H}_2(\mathbf{Z}_1)\|_{max} \leq 15PD^5M_{max}^7$.

For the FFN layer, we define $\mathbf{Y}_2 = \sigma(\mathbf{W}_2^1\mathcal{A}_2(\mathbf{Z}_1) + \mathbf{b}_2^1)$ and $\tilde{\mathbf{Y}}_2 = \sigma(\tilde{\mathbf{W}}_2^1\tilde{\mathcal{A}}_2(\tilde{\mathbf{Z}}_1) + \tilde{\mathbf{b}}_2^1)$, we have

$$\begin{aligned} \|\mathbf{Y}_2\|_{max} &\leq DM_{max}\|\mathcal{A}_2(\mathbf{Z}_1)\|_{max} + M_{max} \leq 16PD^6M_{max}^8, \\ \|\mathbf{Y}_2 - \tilde{\mathbf{Y}}_2\|_{max} &\leq D\delta\|\mathcal{A}_2(\mathbf{Z}_1)\|_{max} + DM_{max}\|\mathcal{A}_2(\mathbf{Z}_1) - \tilde{\mathcal{A}}_2(\tilde{\mathbf{Z}}_1)\|_{max} + \delta \\ &\leq 306031P^3D^{20}M_{max}^{23}\delta. \end{aligned}$$

Let $\mathbf{Z}_2 = \mathcal{F}_2(\mathcal{A}_2(\mathbf{Z}_1))$ and $\tilde{\mathbf{Z}}_2 = \tilde{\mathcal{F}}_2(\tilde{\mathcal{A}}_2(\tilde{\mathbf{Z}}_1))$. Since $d_{\text{ff}}^2 \leq 2D$, it follows that

$$\begin{aligned} \|\mathbf{Z}_2 - \tilde{\mathbf{Z}}_2\|_{\max} &\leq 2D\delta\|\mathbf{Y}_2\|_{\max} + 2DM_{\max}\|\mathbf{Y}_2 - \tilde{\mathbf{Y}}_2\|_{\max} + \delta \\ &\leq 2D\delta(16PD^6M_{\max}^8) + 2DM_{\max}(306031P^3D^{20}M_{\max}^{23}\delta) + \delta \\ &\leq 612095P^3D^{21}M_{\max}^{24}\delta. \end{aligned}$$

The magnitude of the final hidden state is bounded by

$$r_2 := \|\mathbf{Z}_2\|_{\max} \leq 2DM_{\max}\|\mathbf{Y}_2\|_{\max} + M_{\max} \leq 33PD^7M_{\max}^9.$$

Step 3: Readout Layer and Covering Number. The final output is computed by the linear readout vector $c \in \mathbb{R}^{PD}$, where $\|c\|_{\infty} \leq M_{\max}$. The network approximation difference is bounded by

$$\begin{aligned} \|\hat{g}_T(\mathbf{x}; \boldsymbol{\theta}) - \tilde{g}_T(\mathbf{x}; \tilde{\boldsymbol{\theta}})\|_{\infty} &\leq \|c\|_1\|\mathbf{Z}_2 - \tilde{\mathbf{Z}}_2\|_{\max} + \|c - \tilde{c}\|_1\|\tilde{\mathbf{Z}}_2\|_{\max} \\ &\leq (PDM_{\max})(612095P^3D^{21}M_{\max}^{24}\delta) + (PD\delta)(33PD^7M_{\max}^9) \\ &\leq 612128P^4D^{22}M_{\max}^{25}\delta. \end{aligned}$$

This establishes the global Lipschitz constant $L_{\text{param}} = 612128P^4D^{22}M_{\max}^{25}$ with respect to the parameters.

To obtain an η -covering of \mathcal{T} in the function space with respect to the $\|\cdot\|_{\infty}$ norm, it suffices to construct a δ -covering of the parameter space $\Theta = [-M_{\max}, M_{\max}]^{\mathcal{N}_{\text{total}}}$, where $\delta = \eta/L_{\text{param}}$. The covering number of the hypercube Θ is bounded by $(2M_{\max}/\delta)^{\mathcal{N}_{\text{total}}}$. Taking the logarithm yields

$$\log \mathcal{N}(\eta, \mathcal{T}, \|\cdot\|_{\infty}) \leq \mathcal{N}_{\text{total}} \log \left(\frac{2M_{\max}L_{\text{param}}}{\eta} \right) = \mathcal{N}_{\text{total}} \log \left(\frac{1224256P^4D^{22}M_{\max}^{26}}{\eta} \right).$$

This completes the proof. \square

C.2 Deriving learning rates of the ERM algorithm

To establish the generalization bound, we first introduce the following oracle inequality for the ERM algorithm defined over a compact subset of continuous functions.

Lemma 10 ([5], [27]). *Suppose there exist constants $n', \nu > 0$ such that the covering number of the hypothesis space \mathcal{T} satisfies*

$$\log \mathcal{N}(\eta, \mathcal{T}, \|\cdot\|_{\infty}) \leq n' \log \frac{\nu}{\eta}, \quad \forall \eta > 0.$$

Then for any $h^* \in \mathcal{T}$, and any $\eta > 0$, we have

$$\begin{aligned} \text{Prob} \left\{ \|\pi_B f_S - f_{\rho}\|_{\rho}^2 > \eta + 2\|h^* - f_{\rho}\|_{\rho}^2 \right\} &\leq \exp \left\{ n' \log \frac{16\nu B}{\eta} - \frac{3n\eta}{512B^2} \right\} \\ &\quad + \exp \left\{ \frac{-3n\eta^2}{16(3B + \|h^*\|_{\infty})^2(6\|h^* - f_{\rho}\|_{\rho}^2 + \eta)} \right\}. \end{aligned}$$

Utilizing the covering number bounds Lemma 9 established above, we complete the proofs for Theorem 2 and Theorem 4. We optimize the bias-variance trade-off via the oracle inequality Lemma

10 to achieve the final convergence rates.

Proof of Theorem 2. By Theorem 1, for any $\varepsilon \in (0, 1/e]$, there exists a Transformer $h \in \mathcal{T}$ such that $\|h - f_\rho\|_\infty \leq \varepsilon$. Since $\|f_\rho\|_\infty \leq B$, we have $\|h\|_\infty \leq B + \varepsilon \leq B + 1$. By Lemma 9, we have

$$\log \mathcal{N}(\eta, \mathcal{T}, \|\cdot\|_\infty) \leq \mathcal{N}_{total} \log \left(\frac{1224256P^4 D^{22} M_{max}^{26}}{\eta} \right).$$

Substituting $\mathcal{N}_{total} \leq C_N \varepsilon^{-d/\alpha}$, $P \leq C_P \varepsilon^{-d/\alpha}$, $D = d + 4$, and $M_{max} \leq \tilde{C}_{mag} \varepsilon^{-2d/\alpha} \log \frac{1}{\varepsilon}$, we set $n' = C_N \varepsilon^{-d/\alpha}$ and obtain

$$\nu = 1224256(C_P \varepsilon^{-d/\alpha})^4 (d+4)^{22} \left(\tilde{C}_{mag} \varepsilon^{-2d/\alpha} \log \frac{1}{\varepsilon} \right)^{26} \leq C_\nu \varepsilon^{-56d/\alpha} \left(\log \frac{1}{\varepsilon} \right)^{26},$$

where $C_\nu = 1224256C_P^4 (d+4)^{22} \tilde{C}_{mag}^{26}$.

Applying Lemma 10 with $h^* = h$ and $\eta \geq 6\varepsilon^2$, we have

$$\begin{aligned} \text{Prob} \left\{ \|\pi_B f_S - f_\rho\|_\rho^2 > 2\eta \right\} &\leq \exp \left\{ C_N \varepsilon^{-d/\alpha} \log \frac{16\nu B}{\eta} - \frac{3n\eta}{512B^2} \right\} \\ &\quad + \exp \left\{ \frac{-3n\eta^2}{16(4B+1)^2(6\varepsilon^2 + \eta)} \right\}. \end{aligned}$$

For $\eta \geq 6\varepsilon^2$, since $\varepsilon \leq 1/e$, we have $\log \frac{16\nu B}{\eta} \leq (\log \frac{8BC_\nu}{3} + 28 + \frac{56d}{\alpha}) \log \frac{1}{\varepsilon}$. If we further restrict

$$\eta \geq \max \left\{ 6\varepsilon^2, C_1 \frac{\varepsilon^{-d/\alpha} \log \frac{1}{\varepsilon}}{n} \right\}, \quad (11)$$

where $C_1 = \frac{1024B^2 C_N}{3} (\log \frac{8BC_\nu}{3} + 28 + \frac{56d}{\alpha})$, then we have

$$\begin{aligned} &\text{Prob} \left\{ \|\pi_B f_S - f_\rho\|_\rho^2 > 2\eta \right\} \\ &\leq \exp \left\{ C_N \varepsilon^{-d/\alpha} \log \frac{16\nu B}{\eta} - \frac{3n\eta}{512B^2} \right\} + \exp \left\{ \frac{-3n\eta^2}{16(4B+1)^2(6\varepsilon^2 + \eta)} \right\} \\ &\leq \exp \left\{ \frac{3n\eta}{1024B^2} - \frac{3n\eta}{512B^2} \right\} + \exp \left\{ \frac{-3n\eta}{32(4B+1)^2} \right\} \\ &\leq \exp \left\{ -\frac{3n\eta}{1024B^2} \right\} + \exp \left\{ -\frac{3n\eta}{32(4B+1)^2} \right\}, \end{aligned}$$

where the second inequality follows from the restriction (11). Furthermore, by setting $t = 2\eta$ and defining

$$C_3 = \min \left\{ \frac{3}{2048B^2}, \frac{3}{64(4B+1)^2} \right\},$$

we arrive at

$$\text{Prob} \left\{ \|\pi_B f_S - f_\rho\|_\rho^2 > t \right\} \leq 2 \exp(-C_3 n t), \quad \forall t \geq C_2 \max \left\{ \varepsilon^2, \frac{\varepsilon^{-d/\alpha} \log \frac{1}{\varepsilon}}{n} \right\}, \quad (12)$$

where $C_2 = \max\{12, 2C_1\}$. If we apply the formula for the mean of the non-negative random

variable $\xi = \|\pi_B f_S - f_\rho\|_\rho^2$:

$$\mathbb{E}[\xi] = \int_0^\infty \text{Prob}[\xi > t] dt,$$

we see from (12) that with $\Delta := C_2 \max\left\{\varepsilon^2, \frac{\varepsilon^{-d/\alpha} \log \frac{1}{\varepsilon}}{n}\right\}$, there holds

$$\begin{aligned} \mathbb{E}[\|\pi_B f_S - f_\rho\|_\rho^2] &= \left(\int_0^\Delta + \int_\Delta^\infty\right) \text{Prob}\left\{\|\pi_B f_S - f_\rho\|_\rho^2 > t\right\} dt \\ &\leq \Delta + \int_\Delta^\infty 2 \exp(-C_3 n t) dt \\ &\leq \Delta + \frac{2}{C_3 n} \leq C_4 \max\left\{\varepsilon^2, \frac{\varepsilon^{-d/\alpha} \log \frac{1}{\varepsilon}}{n}\right\}, \end{aligned} \quad (13)$$

where $C_4 = C_2 + \frac{2}{C_3}$. Finally, by choosing $\varepsilon = n^{-\frac{\alpha}{2\alpha+d}}$, we obtain

$$\mathbb{E}[\|\pi_B f_S - f_\rho\|_\rho^2] \leq C_4 n^{-\frac{2\alpha}{2\alpha+d}} \log n,$$

Thus, we complete the proof. \square

Proof of Theorem 4. The proof follows the same logic as the proof of Theorem 2, utilizing the covering number bound of \mathcal{T} by Lemma 9, with the approximation complexities from Theorem 3 depending on the intrinsic dimension d :

$$\mathcal{N}_{total} \leq C_N \varepsilon^{-d/\alpha}, \quad P \leq C_P \varepsilon^{-d/\alpha}, \quad M_{max} \leq \tilde{C}_{mag} \varepsilon^{-2d/\alpha} \log \frac{1}{\varepsilon}.$$

If we restrict

$$\eta \geq \max\left\{6\varepsilon^2, C_1 \frac{\varepsilon^{-d/\alpha} \log \frac{1}{\varepsilon}}{n}\right\},$$

where $C_1 = \frac{1024B^2 C_N}{3} (\log \frac{8BC_\nu}{3} + 28 + \frac{56d}{\alpha})$, $C_\nu = 1224256C_P^4 (d+4)^{22} \tilde{C}_{mag}^{26}$, then we have

$$\text{Prob}\left\{\|\pi_B f_S - f_\rho\|_\rho^2 > 2\eta\right\} \leq \exp\left\{-\frac{3n\eta}{1024B^2}\right\} + \exp\left\{-\frac{3n\eta}{32(4B+1)^2}\right\}.$$

Furthermore, setting

$$\tilde{C}_4 = \max\{12, 2C_1\} + 2 \max\left\{\frac{2048B^2}{3}, \frac{64(4B+1)^2}{3}\right\}, \quad (14)$$

we arrive at

$$\mathbb{E}[\|\pi_B f_S - f_\rho\|_\rho^2] \leq \tilde{C}_4 \max\left\{\varepsilon^2, \frac{\varepsilon^{-d/\alpha} \log \frac{1}{\varepsilon}}{n}\right\}.$$

Finally, by choosing $\varepsilon = n^{-\frac{\alpha}{2\alpha+d}}$, we derive

$$\mathbb{E}[\|\pi_B f_S - f_\rho\|_\rho^2] \leq \tilde{C}_4 n^{-\frac{2\alpha}{2\alpha+d}} (\log n),$$

Thus, we complete the proof. □

References

- [1] Yu Bai, Fan Chen, Huan Wang, Caiming Xiong, and Song Mei. Transformers as statisticians: Provable in-context learning with in-context algorithm selection. *Advances in Neural Information Processing Systems*, 36:57125–57211, 2023.
- [2] Tom Brown, Benjamin Mann, Nick Ryder, Melanie Subbiah, Jared D Kaplan, Prafulla Dhariwal, Arvind Neelakantan, Pranav Shyam, Girish Sastry, Amanda Askell, et al. Language models are few-shot learners. In *Advances in Neural Information Processing Systems*, volume 33, pages 1877–1901, 2020.
- [3] Minshuo Chen, Haoming Jiang, Wenjing Liao, and Tuo Zhao. Efficient approximation of deep relu networks for functions on low dimensional manifolds. *Advances in Neural Information Processing Systems*, 32, 2019.
- [4] Minshuo Chen, Haoming Jiang, Wenjing Liao, and Tuo Zhao. Nonparametric regression on low-dimensional manifolds using deep relu networks: Function approximation and statistical recovery. *Information and Inference: A Journal of the IMA*, 11(4):1203–1253, 2022.
- [5] Charles K Chui, Shao-Bo Lin, and Ding-Xuan Zhou. Deep net tree structure for balance of capacity and approximation ability. *Frontiers in Applied Mathematics and Statistics*, 5:46, 2019.
- [6] Alexander Cloninger and Timo Klock. A deep network construction that adapts to intrinsic dimensionality beyond the domain. *Neural Networks*, 141:404–419, 2021.
- [7] Felipe Cucker and Ding Xuan Zhou. *Learning Theory: An Approximation Theory Viewpoint*, volume 24. Cambridge University Press, 2007.
- [8] Biraj Dahal, Alexander Havrilla, Minshuo Chen, Tuo Zhao, and Wenjing Liao. On deep generative models for approximation and estimation of distributions on manifolds. *Advances in Neural Information Processing Systems*, 35:10615–10628, 2022.
- [9] Qingxiu Dong, Lei Li, Damai Dai, Ce Zheng, Jingyuan Ma, Rui Li, Heming Xia, Jingjing Xu, Zhiyong Wu, Baobao Chang, et al. A survey on in-context learning. In *Proceedings of the 2024 Conference on Empirical Methods in Natural Language Processing*, pages 1107–1128, 2024.
- [10] Alexey Dosovitskiy, Lucas Beyer, Alexander Kolesnikov, Dirk Weissenborn, Xiaohua Zhai, Thomas Unterthiner, Mostafa Dehghani, Matthias Minderer, Georg Heigold, Sylvain Gelly, et al. An image is worth 16x16 words: Transformers for image recognition at scale. In *International Conference on Learning Representations*, 2021.
- [11] Benjamin L Edelman, Surbhi Goel, Sham Kakade, and Cyril Zhang. Inductive biases and variable creation in self-attention mechanisms. In *International Conference on Machine Learning*, pages 5793–5831. PMLR, 2022.
- [12] Herbert Federer. Curvature measures. *Transactions of the American Mathematical Society*, 93(3):418–491, 1959.

- [13] Shivam Garg, Dimitris Tsipras, Percy S Liang, and Gregory Valiant. What can transformers learn in-context? a case study of simple function classes. *Advances in Neural Information Processing Systems*, 35:30583–30598, 2022.
- [14] Christopher R Genovese, Marco Perone Pacifico, Isabella Verdinelli, Larry Wasserman, et al. Minimax manifold estimation. *Journal of Machine Learning Research*, 13:1263–1291, 2012.
- [15] Ian J Goodfellow, Jean Pouget-Abadie, Mehdi Mirza, Bing Xu, David Warde-Farley, Sherjil Ozair, Aaron Courville, and Yoshua Bengio. Generative adversarial nets. *Advances in Neural Information Processing Systems*, 27, 2014.
- [16] Alex Graves, Abdel-rahman Mohamed, and Geoffrey Hinton. Speech recognition with deep recurrent neural networks. In *2013 IEEE International Conference on Acoustics, Speech and Signal Processing*, pages 6645–6649. Ieee, 2013.
- [17] Iryna Gurevych, Michael Kohler, and Gözde Gül Şahin. On the rate of convergence of a classifier based on a transformer encoder. *IEEE Transactions on Information Theory*, 68(12):8139–8155, 2022.
- [18] Alex Havrilla and Wenjing Liao. Understanding scaling laws with statistical and approximation theory for transformer neural networks on intrinsically low-dimensional data. *Advances in Neural Information Processing Systems*, 37:42162–42210, 2024.
- [19] Haotian Jiang and Qianxiao Li. Approximation rate of the transformer architecture for sequence modeling. *Advances in Neural Information Processing Systems*, 37:68926–68955, 2024.
- [20] Yuling Jiao, Yanming Lai, Yang Wang, and Bokai Yan. Transformers can overcome the curse of dimensionality: A theoretical study from an approximation perspective. *Journal of Machine Learning Research*, 27(50):1–34, 2026.
- [21] Tokio Kajitsuka and Issei Sato. Are transformers with one layer self-attention using low-rank weight matrices universal approximators? In *The Twelfth International Conference on Learning Representations*, 2024.
- [22] Alex Krizhevsky, Ilya Sutskever, and Geoffrey E Hinton. Imagenet classification with deep convolutional neural networks. *Advances in Neural Information Processing Systems*, 25, 2012.
- [23] John M Lee. *Riemannian Manifolds: An Introduction to Curvature*. Springer Science & Business Media, 2006.
- [24] Hao Liu, Minshuo Chen, Tuo Zhao, and Wenjing Liao. Besov function approximation and binary classification on low-dimensional manifolds using convolutional residual networks. In *International Conference on Machine Learning*, pages 6770–6780. PMLR, 2021.
- [25] Hao Liu, Alex Havrilla, Rongjie Lai, and Wenjing Liao. Deep nonparametric estimation of intrinsic data structures by chart autoencoders: Generalization error and robustness. *Applied and Computational Harmonic Analysis*, 68:101602, 2024.
- [26] Pengfei Liu, Weizhe Yuan, Jinlan Fu, Zhengbao Jiang, Hiroaki Hayashi, and Graham Neubig. Pre-train, prompt, and predict: A systematic survey of prompting methods in natural language processing. *ACM Computing Surveys*, 55(9):1–35, 2023.

- [27] Tong Mao, Zhongjie Shi, and Ding-Xuan Zhou. Theory of deep convolutional neural networks iii: Approximating radial functions. *Neural Networks*, 144:778–790, 2021.
- [28] John Moody and Christian J Darken. Fast learning in networks of locally-tuned processing units. *Neural Computation*, 1(2):281–294, 1989.
- [29] Ryumei Nakada and Masaaki Imaizumi. Adaptive approximation and generalization of deep neural network with intrinsic dimensionality. *Journal of Machine Learning Research*, 21(174):1–38, 2020.
- [30] Partha Niyogi, Stephen Smale, and Shmuel Weinberger. Finding the homology of submanifolds with high confidence from random samples. *Discrete & Computational Geometry*, 39(1):419–441, 2008.
- [31] Long Ouyang, Jeffrey Wu, Xu Jiang, Diogo Almeida, Carroll Wainwright, Pamela Mishkin, Chong Zhang, Sandhini Agarwal, Katarina Slama, Alex Ray, et al. Training language models to follow instructions with human feedback. *Advances in Neural Information Processing Systems*, 35:27730–27744, 2022.
- [32] Johannes Schmidt-Hieber. Nonparametric regression using deep neural networks with ReLU activation function. *The Annals of Statistics*, 48(4):1875–1897, 2020.
- [33] Zhaiming Shen, Alexander Hsu, Rongjie Lai, and Wenjing Liao. Understanding in-context learning on structured manifolds: Bridging attention to kernel methods. In *The Fourteenth International Conference on Learning Representations*, 2026.
- [34] Donald Shepard. A two-dimensional interpolation function for irregularly-spaced data. In *Proceedings of the 1968 23rd ACM National Conference*, pages 517–524, 1968.
- [35] Zhongjie Shi, Jun Fan, Linhao Song, Ding-Xuan Zhou, and Johan AK Suykens. Nonlinear functional regression by functional deep neural network with kernel embedding. *Journal of Machine Learning Research*, 26(284):1–49, 2025.
- [36] Zhongjie Shi, Zhiying Fang, and Yuan Cao. Approximation and estimation capability of vision transformers for hierarchical compositional models. *Applied and Computational Harmonic Analysis*, page 101849, 2025.
- [37] Zhongjie Shi, Fanghui Liu, Yuan Cao, and Johan AK Suykens. Can overfitted deep neural networks in adversarial training generalize? an approximation viewpoint. *SIAM Journal on Mathematics of Data Science*, 8(2):225–256, 2026.
- [38] Zhongjie Shi, Zhan Yu, and Ding-Xuan Zhou. Learning theory of distribution regression with neural networks. *Constructive Approximation*, 62(1):61–104, 2025.
- [39] David Silver, Julian Schrittwieser, Karen Simonyan, Ioannis Antonoglou, Aja Huang, Arthur Guez, Thomas Hubert, Lucas Baker, Matthew Lai, Adrian Bolton, et al. Mastering the game of go without human knowledge. *Nature*, 550(7676):354–359, 2017.
- [40] Yang Song, Jascha Sohl-Dickstein, Diederik P Kingma, Abhishek Kumar, Stefano Ermon, and Ben Poole. Score-based generative modeling through stochastic differential equations. In *International Conference on Learning Representations*, 2021.

- [41] Shokichi Takakura and Taiji Suzuki. Approximation and estimation ability of transformers for sequence-to-sequence functions with infinite dimensional input. In *International Conference on Machine Learning*, pages 33416–33447. PMLR, 2023.
- [42] Loring W Tu. Manifolds. In *An Introduction to Manifolds*, pages 47–83. Springer, 2011.
- [43] Ashish Vaswani, Noam Shazeer, Niki Parmar, Jakob Uszkoreit, Llion Jones, Aidan N Gomez, Łukasz Kaiser, and Illia Polosukhin. Attention is all you need. *Advances in Neural Information Processing Systems*, 30, 2017.
- [44] Colin Wei, Yining Chen, and Tengyu Ma. Statistically meaningful approximation: a case study on approximating turing machines with transformers. In *Advances in Neural Information Processing Systems*, volume 35, pages 12071–12083, 2022.
- [45] Dmitry Yarotsky. Error bounds for approximations with deep relu networks. *Neural Networks*, 94:103–114, 2017.
- [46] Dmitry Yarotsky. Optimal approximation of continuous functions by very deep relu networks. In *Conference on Learning Theory*, pages 639–649. PMLR, 2018.
- [47] Chulhee Yun, Srinadh Bhojanapalli, Ankit Singh Rawat, Sashank J Reddi, and Sanjiv Kumar. Are transformers universal approximators of sequence-to-sequence functions? In *International Conference on Learning Representations*, 2020.
- [48] Chulhee Yun, Yin-Wen Chang, Srinadh Bhojanapalli, Ankit Singh Rawat, Sashank Reddi, and Sanjiv Kumar. $O(n)$ connections are expressive enough: Universal approximability of sparse transformers. In *Advances in Neural Information Processing Systems*, volume 33, pages 13783–13794, 2020.
- [49] Manzil Zaheer, Guru Guruganesh, Kumar Avinava Dubey, Joshua Ainslie, Chris Alberti, Santiago Ontanon, Philip Pham, Anirudh Ravula, Qifan Wang, Li Yang, et al. Big bird: Transformers for longer sequences. In *Advances in Neural Information Processing Systems*, volume 33, pages 17283–17297, 2020.
- [50] Yufeng Zhang, Boyi Liu, Qi Cai, Lingxiao Wang, and Zhaoran Wang. An analysis of attention via the lens of exchangeability and latent variable models. *arXiv preprint arXiv:2212.14852*, 2022.